Photometric Reverberation Mapping of Hα emission line in Nearby Seyfert Galaxies

CATALINA SOBRINO FIGAREDO[1,2,3] DORON CHELOUCHE[1,2] MARTIN HAAS[3] SHAY ZUCKER[4] SHAI KASPI[5]
MARTIN W. OCHMANN[3,6] ROLF CHINI[3,7,8] MALTE A. PROBST[6] WOLFRAM KOLLATSCHNY[6]

[1]Department of Physics, Faculty of Natural Sciences, University of Haifa, Haifa 3498838, Israel
[2]Haifa Research Center for Theoretical Physics and Astrophysics, University of Haifa, Haifa 3498838, Israel
[3]Ruhr University Bochum, Faculty of Physics and Astronomy, Astronomical Institute (AIRUB), 44780 Bochum, Germany
[4]Department of Geosciences, Raymond and Beverly Sackler Faculty of Exact Sciences, Tel Aviv University, Tel Aviv 6997801, Israel
[5]School of Physics and Astronomy and Wise Observatory, Raymond and Beverly Sackler Faculty of Exact Sciences, Tel-Aviv University, Tel-Aviv 6997801, Israel
[6]Institut fur Astrophysik und Geophysik, Universitat Gottingen, Friedrich-Hund Platz 1, D-37077 Gottingen, Germany
[7]Universidad Cato´lica del Norte, Instituto de Astronom´ıa, Avenida Angamos 0610, Antofagasta, Chile
[8]Polish Academy of Sciences, Nicolaus Copernicus Astronomical Center, Bartycka 18, 00-716 Warszawa, Poland

Szczecin 2024

אוניברסיטת חיפה
University of Haifa
جامعة حيفا

Outline

- **Introduction:** AGN, Reverberation Mapping and radius-Luminosity relation
- **Observations:** Sample and Data quality
- **Methods:** Time delay determination, BH estimation, AGN Luminosity
- **Results:** BLR sizes, AGN Luminosities and Accretion Rate
- **Radius-Luminosity Relation:** Hα r-L results and comments on the scatter
- **Summary**

Introduction

<u>AGN Model:</u> SMBH, AD, BLR

<u>Method:</u> Reverberation Mapping
- monitor AGN variability
- measure time delays between changes in the continuum and line emission

<u>Applications:</u>
- Galaxy evolution, growth and distribution of BH

<u>BLR Radius - Luminosity relation:</u>
- Hβ emission line best studied (~120 sources)

$$R_{\mathrm{BLR}} \propto L^{\beta};\, \beta \sim 0.5$$ (Bentz+13)

- exact slope unclear
- significant scatter in the relation
- accretion rate dependence
- used for BH mass estimation

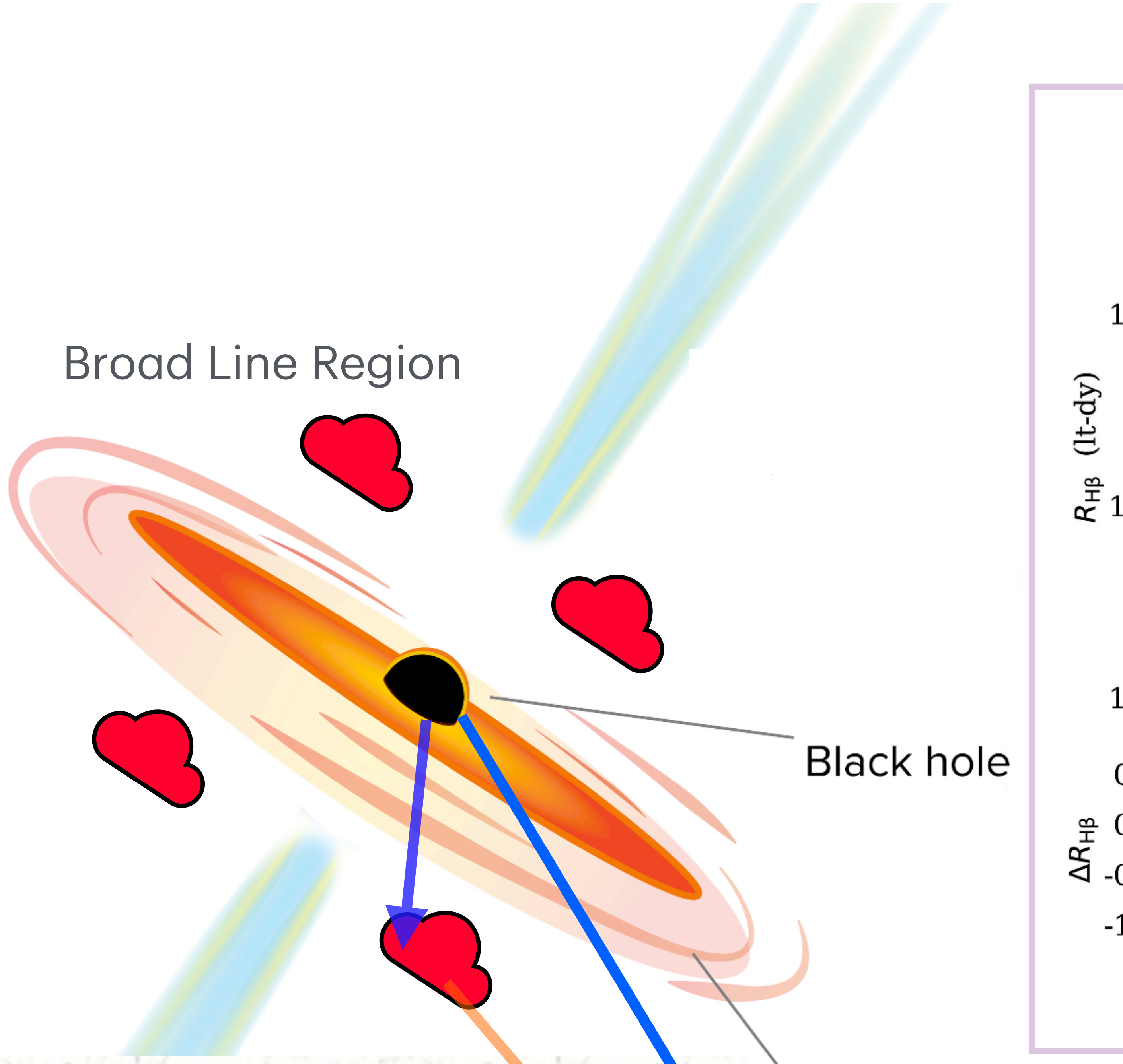

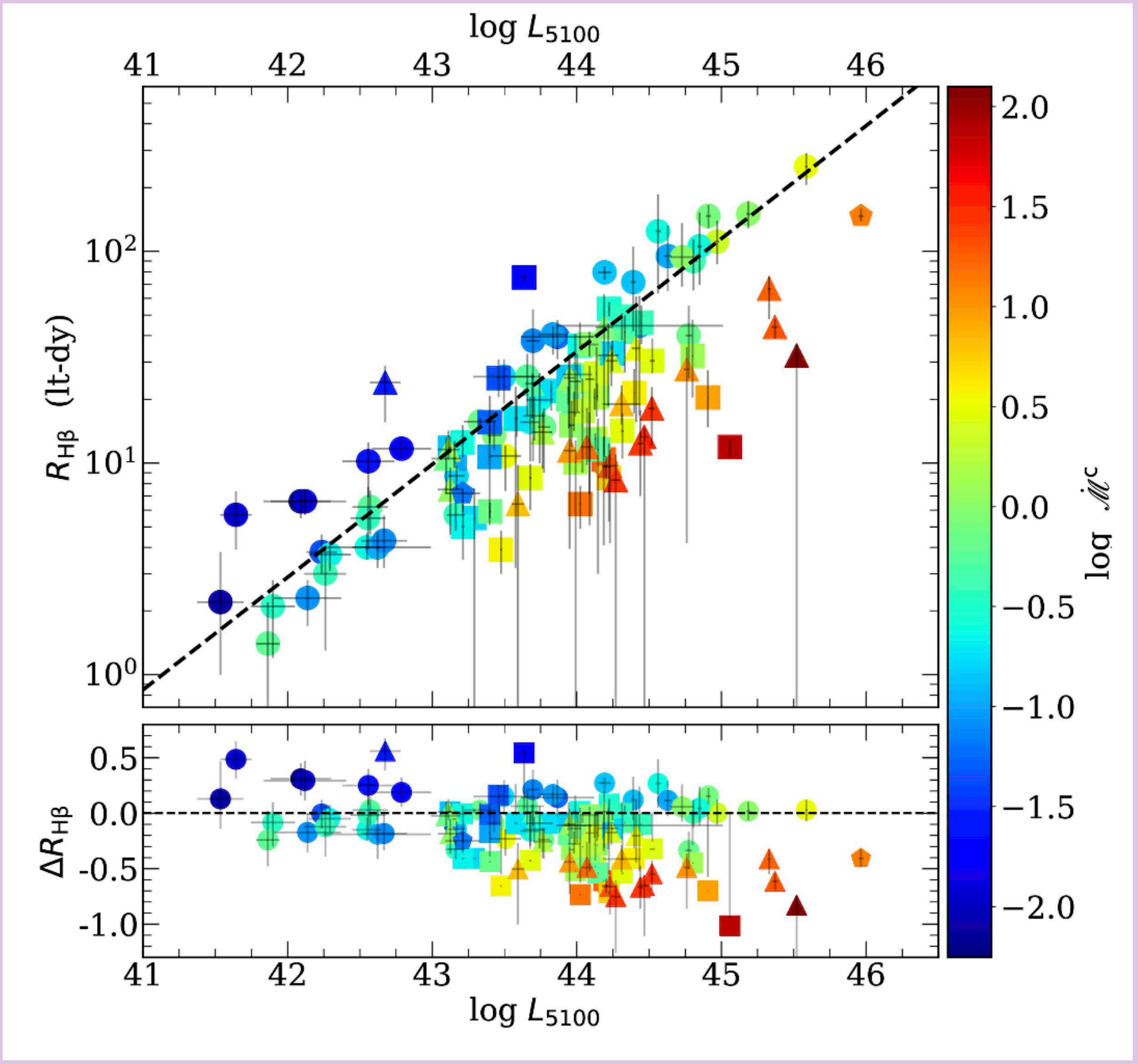

(Martinez-Aldama+19)

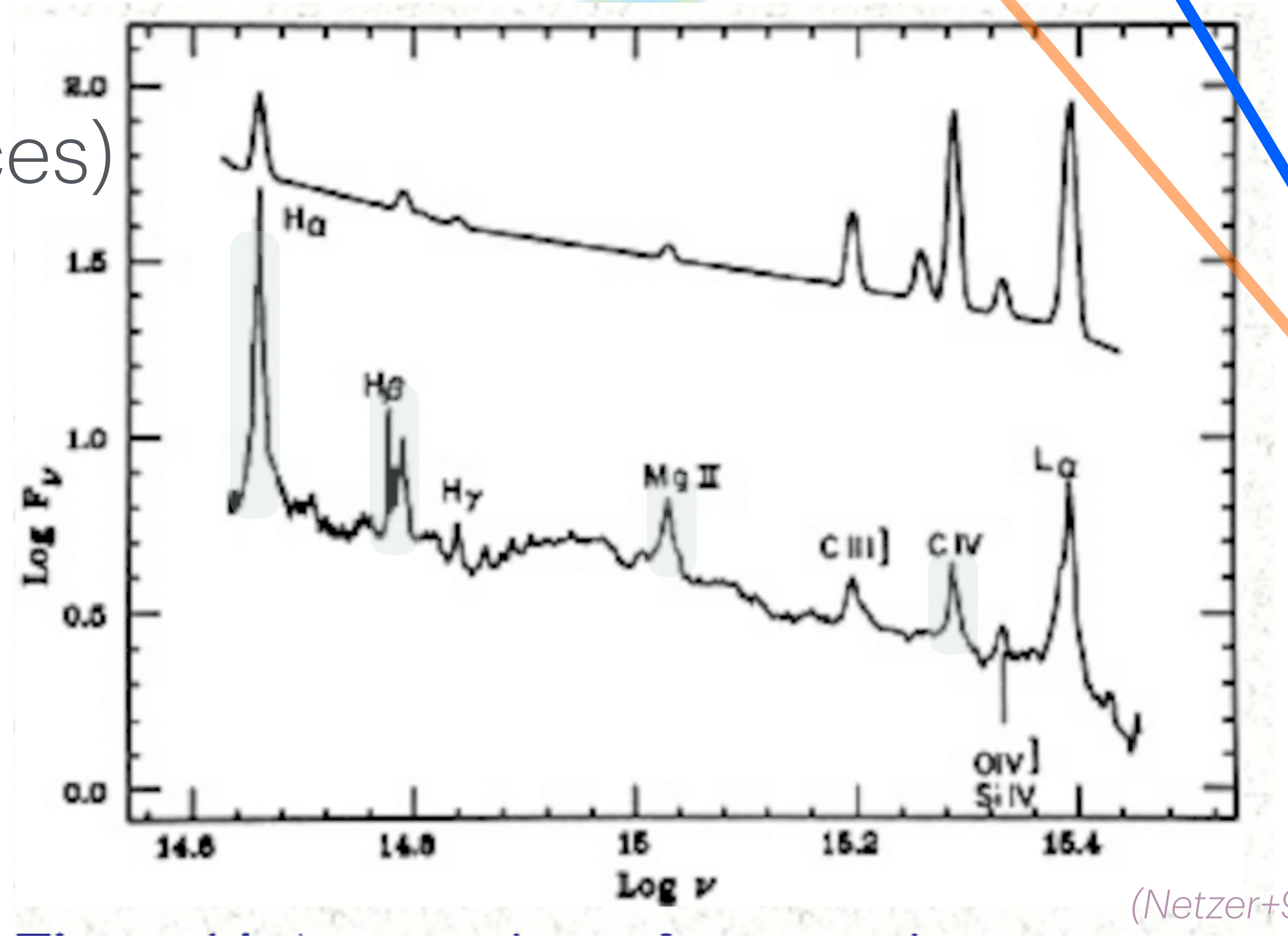

(Netzer+90)

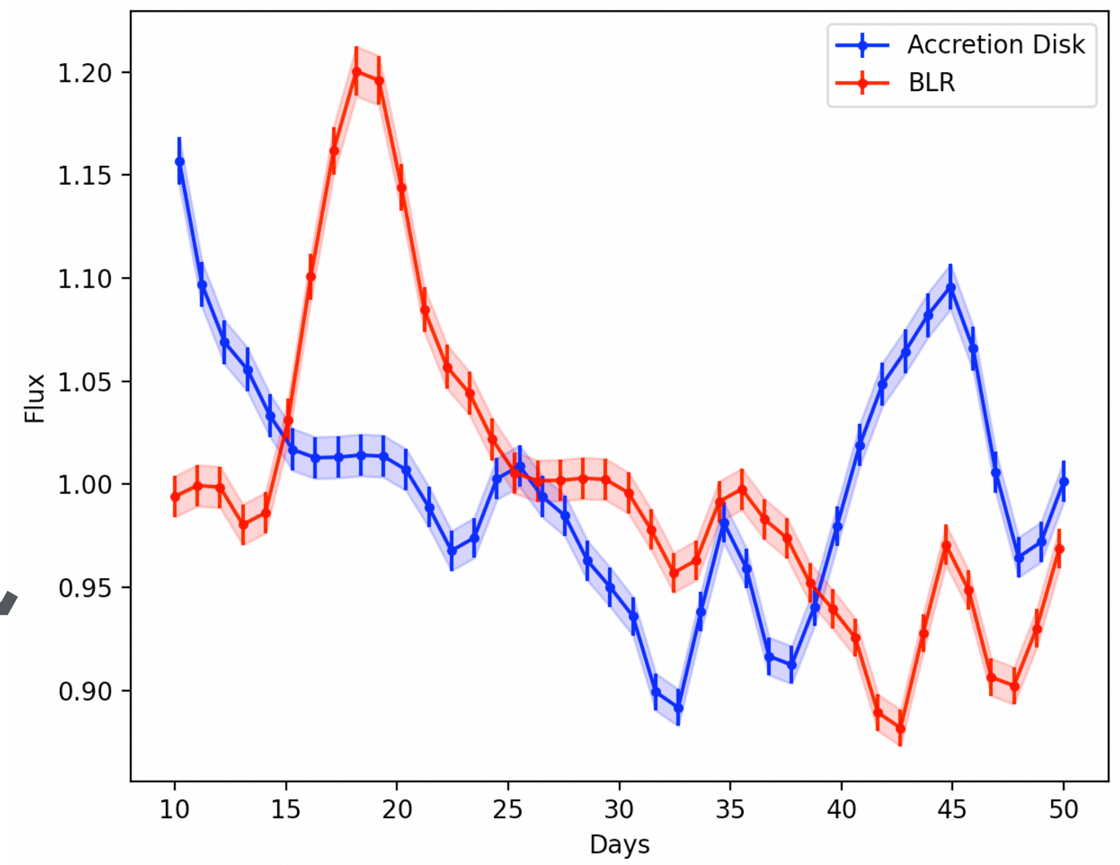

Observations

<u>Sample of ~ 80 AGN:</u>

- Seyfert Galaxies from Veron-Cetty Catalog *(VC&V+10)*
- Nearby AGN redshift between 0.01 and 0.05
- Vmag < 16
- Maximal expected delay < 100 days (r-L relation)

<u>Settings:</u>

- Continuum: Broad band *BV* filters
- BLR: Narrow band filters centered at 670, 680 or 690 nm, covering the broad Hα emission line

<u>Observations:</u>

- 3 optical telescopes: v6(15cm), BESTII(25cm), v16(40cm)
- Planned monitored campaign ~ 6 months
- Optical monitoring during years 2011-2018

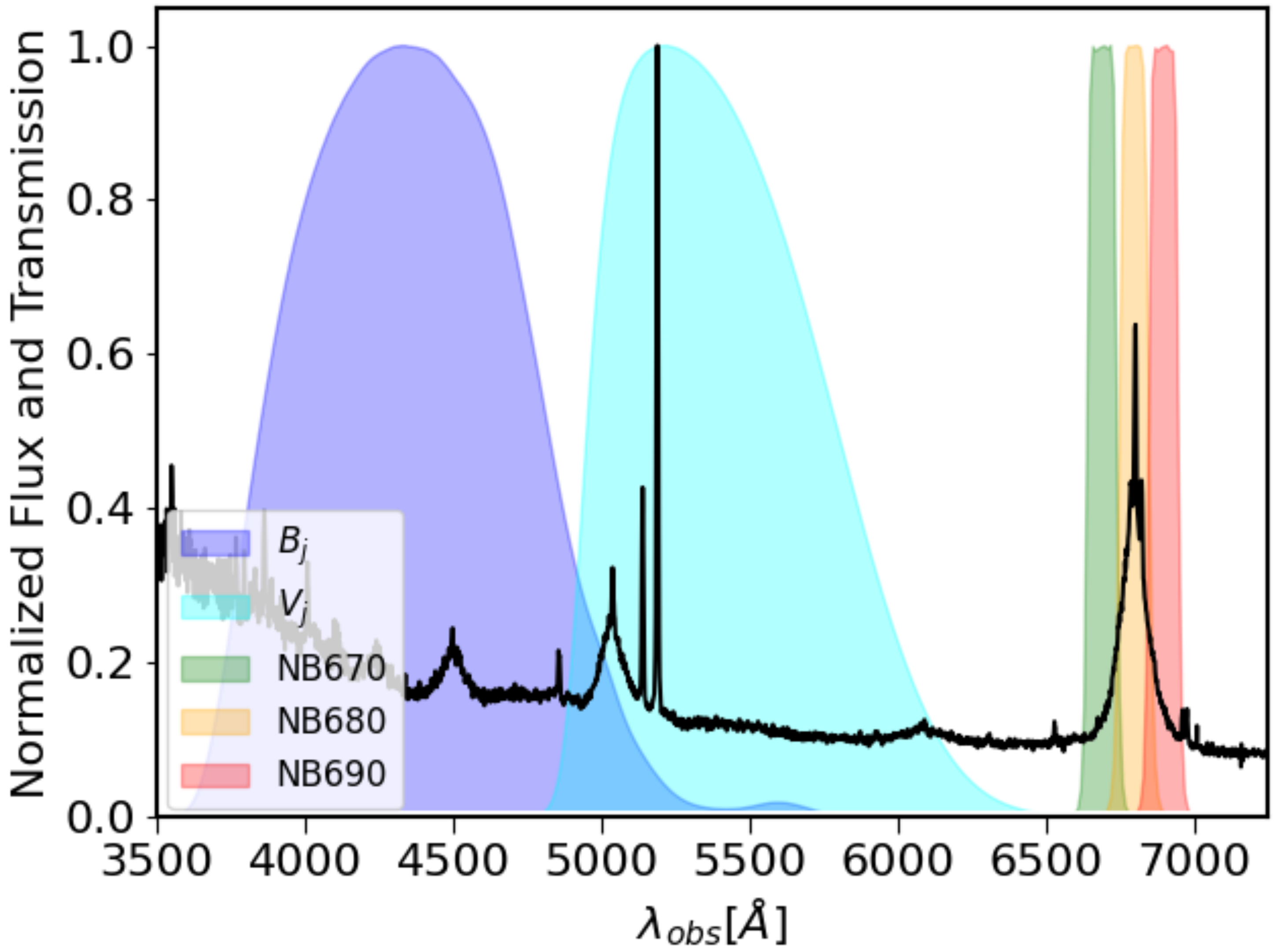

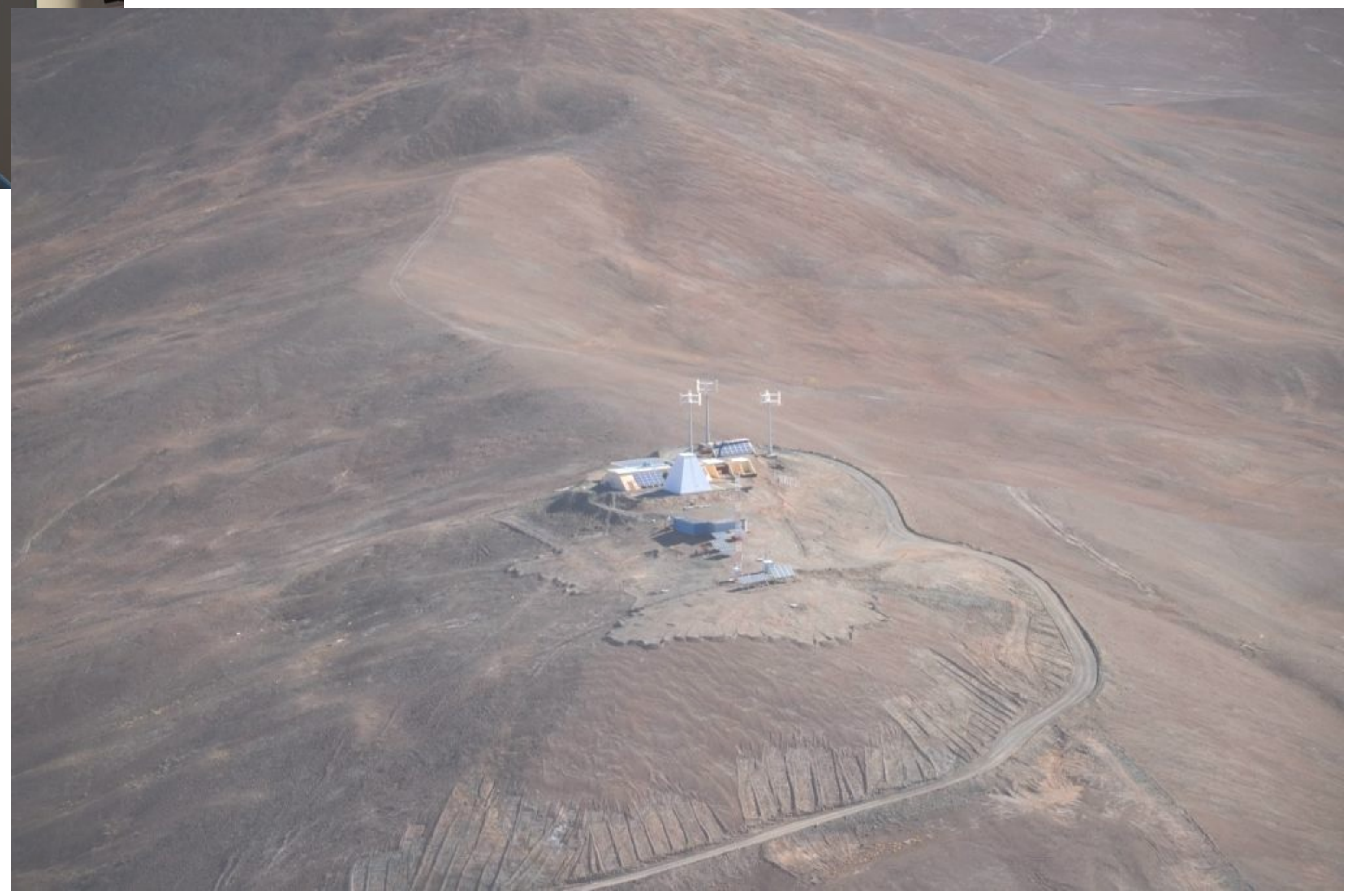

Observations

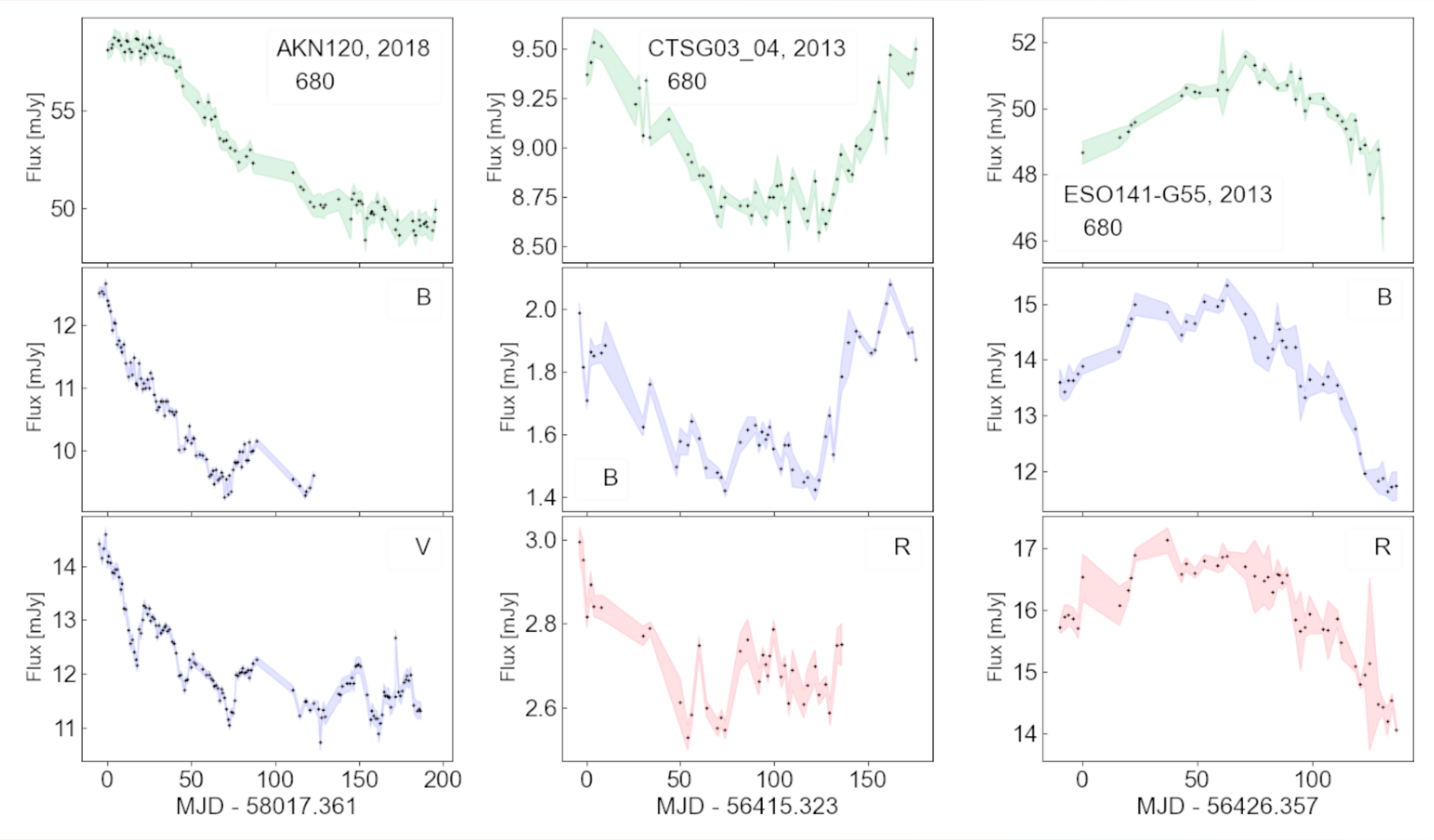

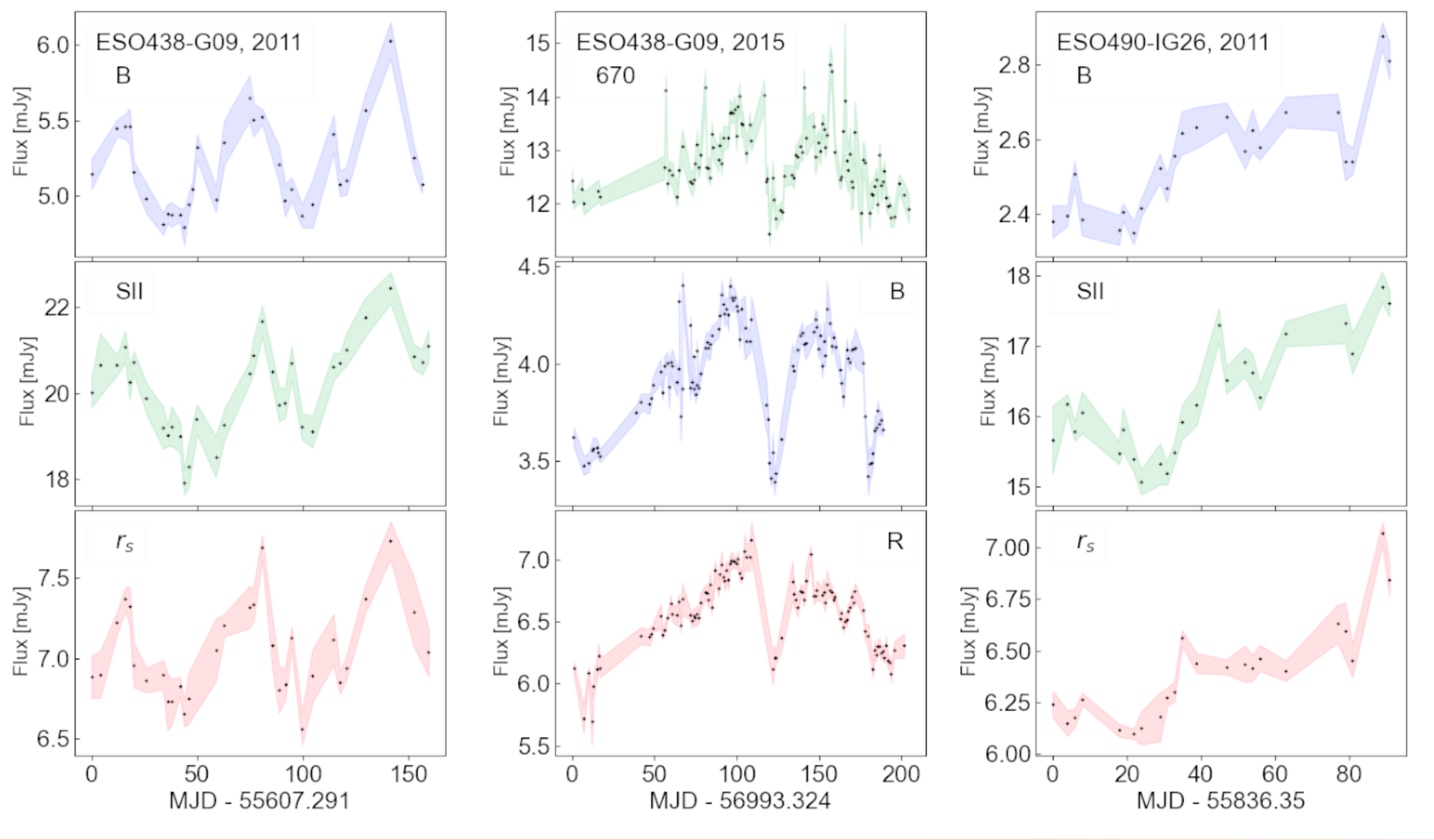

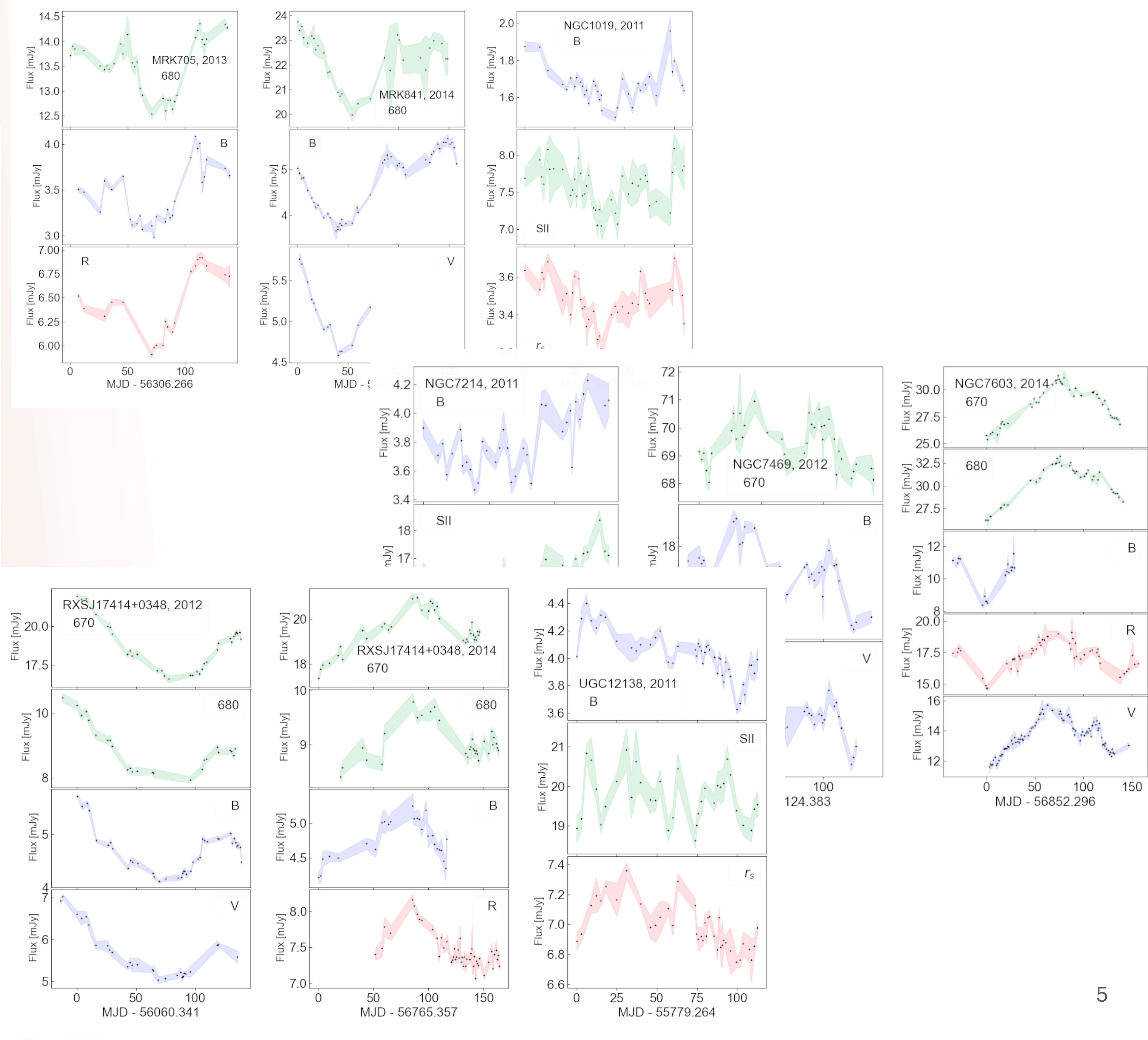

Observations

Data Screening:

- Weather conditions and occasional telescope issues
- Duration: Long enough light curves compared to expected delay
  optimal: 3 times larger than delay
- Cadence: ensure well-sampled light curves

Light curve Variability:

- Fractional variability $F_{\rm var}$ and variance s^2: quantify the intrinsic AGN variability and discard low variability $F_{\rm var}$<0.01

Light curve Quality:

- Von Neumann estimator ($\sigma^2_{\rm VN}$) - check randomness of the light curves and ensure reliable variability patterns

- Ratio $\eta = \sigma^2_{\rm VN}/s^2$: estimation quality of light curve

Screened final AGN Sample: 48 AGN

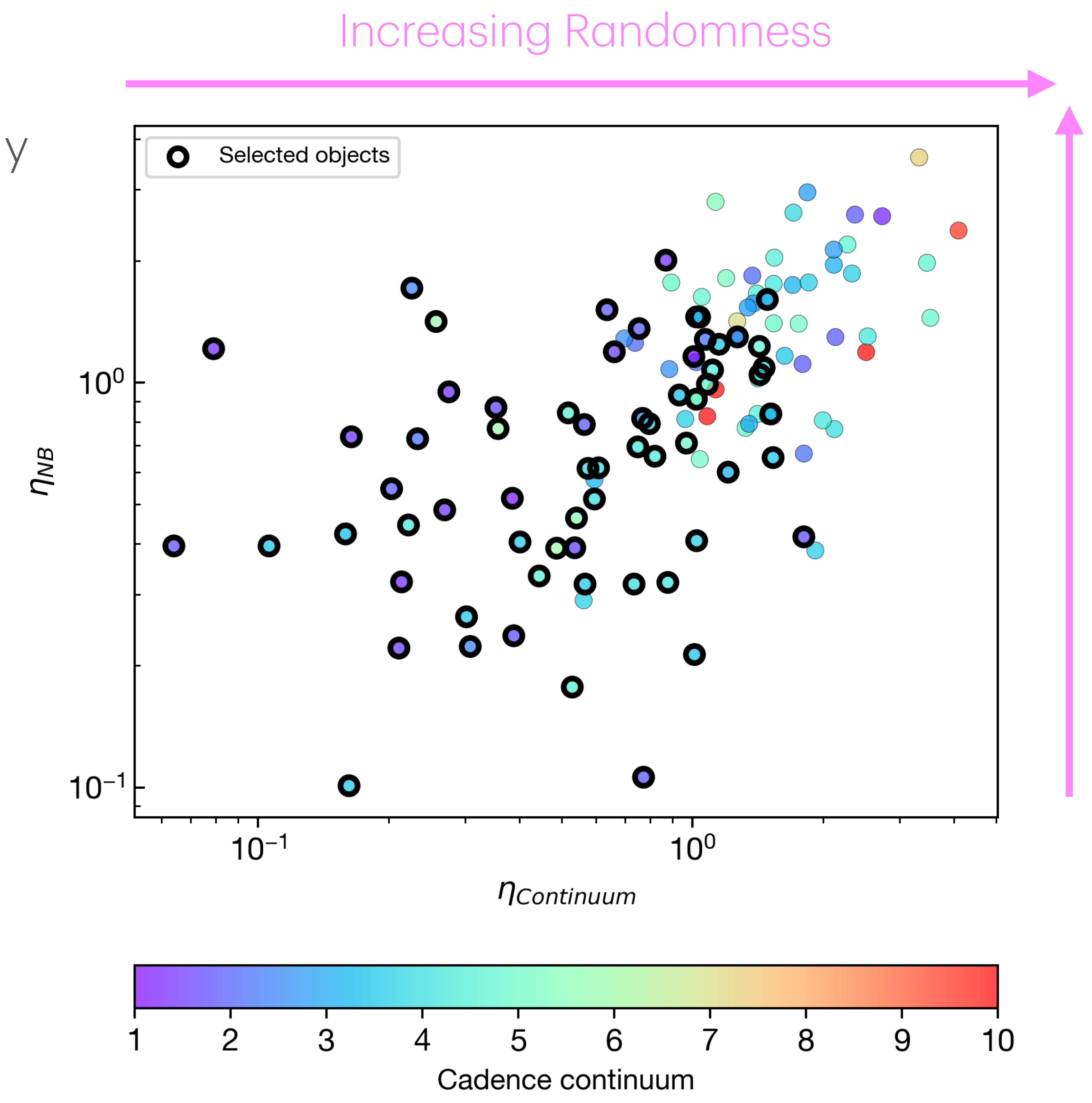

Object	z[1]	D_L[1] [Mpc]	RA h	RA min	RA sec	DEC °	DEC ′	DEC ″	Type[2]	Vmag[2]
HE0003-5023	0.0345	149	0	05	43.1	-50	06	55	S1	14
MRK335	0.02578	111	0	06	19.5	+20	12	11	NLS1	13.85
WPVS_7	0.02861	127	0	39	15.9	-51	17	1.5	NLS1	15.28
IRAS01089-4743	0.02392	105	01	11	09.7	-47	27	37.23	S1	14.53
NGC985	0.04314	193	02	34	37.7	-08	47	15.44	S1.5	14.28
NGC1019	0.02434	106	02	38	27.4	+01	54	28	S1.5	14.95
ESO549-G49	0.02627	117	04	02	25.8	-18	02	52	S1	14.2
3C120	0.03301	149	04	33	11.1	+05	21	15	S1.5	15.05
MCG-02.12.050	0.03600	164	04	38	14.1	-10	47	45	S1	15
AKN120	0.03271	148	05	16	11.4	+00	08	59	S1	14.59
RXSJ06225-2317	0.03778	174	06	22	33.4	-23	17	42	S1	14.85
ESO490-IG26	0.02485	114	06	40	11.8	-25	53	38	S1	15
MRK705	0.02879	135	09	26	3.3	+12	44	3	S1.2	14.6
MRK1239	0.01993	94.7	09	52	19.1	+01	36	44	NLS1	14.39
WPVS48	0.0370	173	09	59	42.6	-31	12	59	NLS1	14.78
IRAS09595-0755	0.055	246.9	10	02	0.1	-08	09	41	S1	14.64
ESO374-G25	0.02367	111	10	03	23.6	-37	33	39	S1	15.29
RX J1103.2-0654	0.02606	123	11	03	15.8	-06	54	10	S1	13.34
ESO438-G09	0.02401	113	11	10	48	-28	30	4	S1	14.17
HE1136-2304	0.0270	127	11	38	51.2	-23	21	35	CL	17.4
HE1143-1810	0.03295	155	11	45	40.4	-18	27	15.51	S1.5	14.7*
PG1149-110	0.0490	230	11	52	3.5	-11	22	23	S1.2	15.46
NGC4726	0.02543	120	12	51	32.3	-14	13	17	S1	14.2
ESO323-G77	0.01501	71.3	13	06	26.2	-40	24	52	S1.2	13.42
MRK1347	0.04995	234	13	22	55.5	+08	09	42	S1	14.59
IC4329A	0.01605	75.9	13	49	19.3	-30	18	34	S1.2	13.66
ESO578-G09	0.03502	163	13	56	36.7	-19	31	44	S1	15.2
PGC50427	0.02346	109	14	08	6.7	-30	23	53	S1.5	15.3
ESO511-G030	0.02239	104	14	19	22.3	-26	38	41	S1	14.9
MRK841	0.03642	168	15	04	1.2	+10	26	16	S1.5	14.27
NGC5940	0.03408	157	15	31	18.1	+07	27	27	S1	14.9
RXSJ17414+0348	0.0230	103	17	41	28.1	+03	48	51	S1	15.3
MCG+03-47-002	0.04000	180	18	27	14.7	+19	56	19.0	S1	15.3
ESO141-G55	0.03711	168	19	21	14.3	-58	40	13	S1.2	13.64
CTSG03_04	0.04002	181	19	38	04.3	-51	09	49.6	S1.2	15.2
ESO399-IG20	0.0250	110	20	06	58.1	-34	32	55	NLS1	14.51
NGC6860	0.01488	65.3	20	08	47.1	-61	06	0	S1.5	13.53
PGC64989	0.01937	83.5	20	34	31.4	-30	37	29	S1	13.3
MRK509	0.0344	152	20	44	9.7	-10	43	24.5	S1.5	13.2
1H2107-097	0.02698	117	21	09	9.9	-09	40	15	S1.2	14.39
HE2128-0221	0.05248	236	21	30	49.9	-02	08	14.7	S1	17.4*
NGC7214	0.02385	103	22	09	07.6	-27	48	34.1	S1.2	14.10
UGC12138	0.02509	107	22	40	17.0	+08	03	14.09	S1.8	14.45
NGC7469	0.01627	67.2	23	03	15.6	+08	52	26.39	S1.5	13.04
F1041	0.03347	148	23	17	30.2	-42	47	05.3	S1	15.2
NGC7603	0.02876	124	23	18	56.6	+00	14	38	S1.5	14.01
IRAS23226-3843	0.03590	159	23	25	24.2	-38	26	49.2	S1	14.24
UM163	0.03343	146	23	39	32.3	-02	27	45	S1.5	14.86

Screened final AGN Sample: 48 AGN

Methods

Time delay determination: τ-α formalism

Assumption:

- BLR variability model = combination of continuum and a lagging component that contributes by a factor of α to the band
- α takes values between 0 and 1
  - α = 0 (no varying component in the line)
  - α = 1 (pure emission line)

Calculation:

- 2D Pearson correlation coefficient: $r(\tau, \alpha)$
- Searching for maximal $r(\tau, \alpha)$ requiring $\partial r(\tau, \alpha)/\partial \alpha = 0$
- Correlation coefficient $r_e(\tau)$ easy to implement: combination of correlation and autocorrelation functions
- Final lag t: delay τ which maximize $r_e(\tau)$ and $(0 \leq \alpha \leq 1)$

Result:

- Decomposition between continuum and emission line at the light curve level, without previous spectral knowledge

$$f_{lc}^{m}(t) = (1-\alpha) f_c(t) + \alpha f_c(t-\tau).$$

$$r(\tau, \alpha) = \frac{(1-\alpha)\mathrm{CCF}(0) + \alpha \mathrm{CCF}(\tau)}{\sqrt{1 - 2\alpha + 2\alpha^2 + 2\alpha(1-\alpha)\mathrm{ACF}_c(\tau)}}$$

$$\alpha(\tau) = \frac{\mathrm{CCF}(0)\mathrm{ACF}_c(\tau) - \mathrm{CCF}(\tau)}{[\mathrm{CCF}(\tau) + \mathrm{CCF}(0)][\mathrm{ACF}_c(\tau) - 1]}.$$

$$r_e(\tau) = \sqrt{\frac{\mathrm{CCF}^2(0) - 2\mathrm{CCF}(0)\mathrm{CCF}(\tau)\mathrm{ACF}_c(\tau) + \mathrm{CCF}^2(\tau)}{1 - \mathrm{ACF}_c^2(\tau)}}.$$

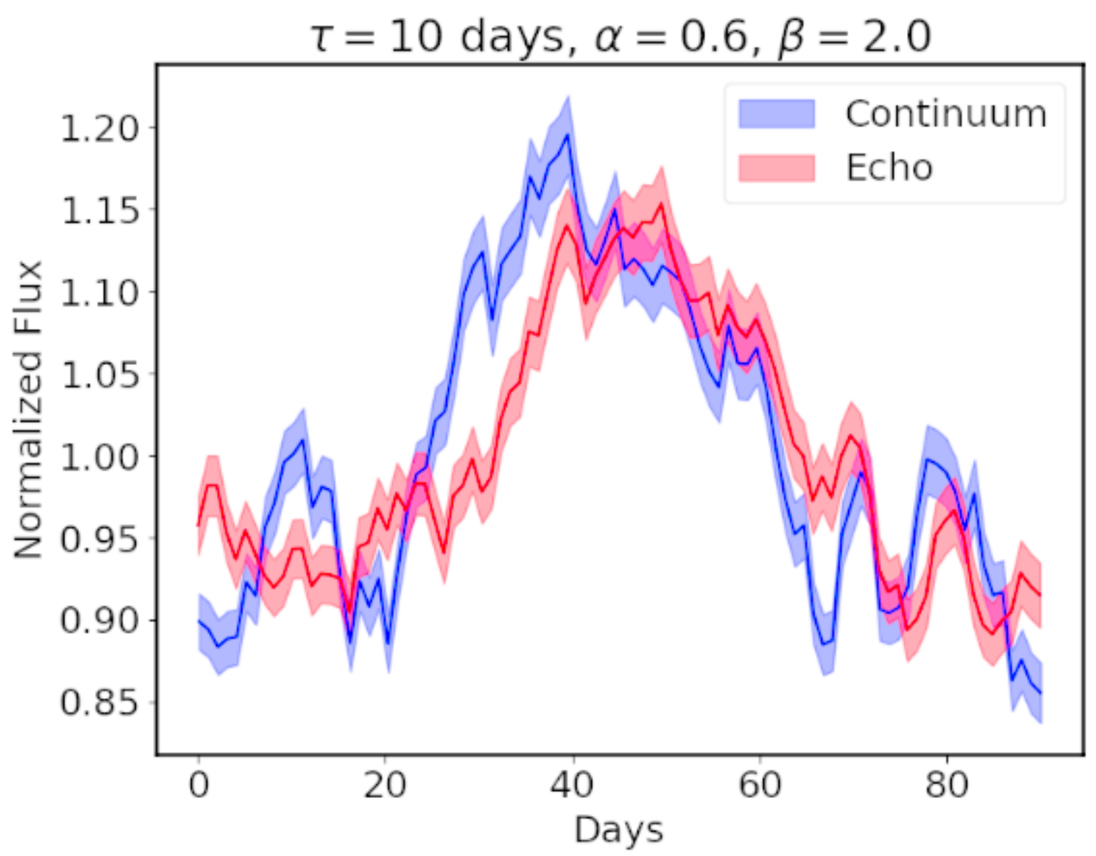

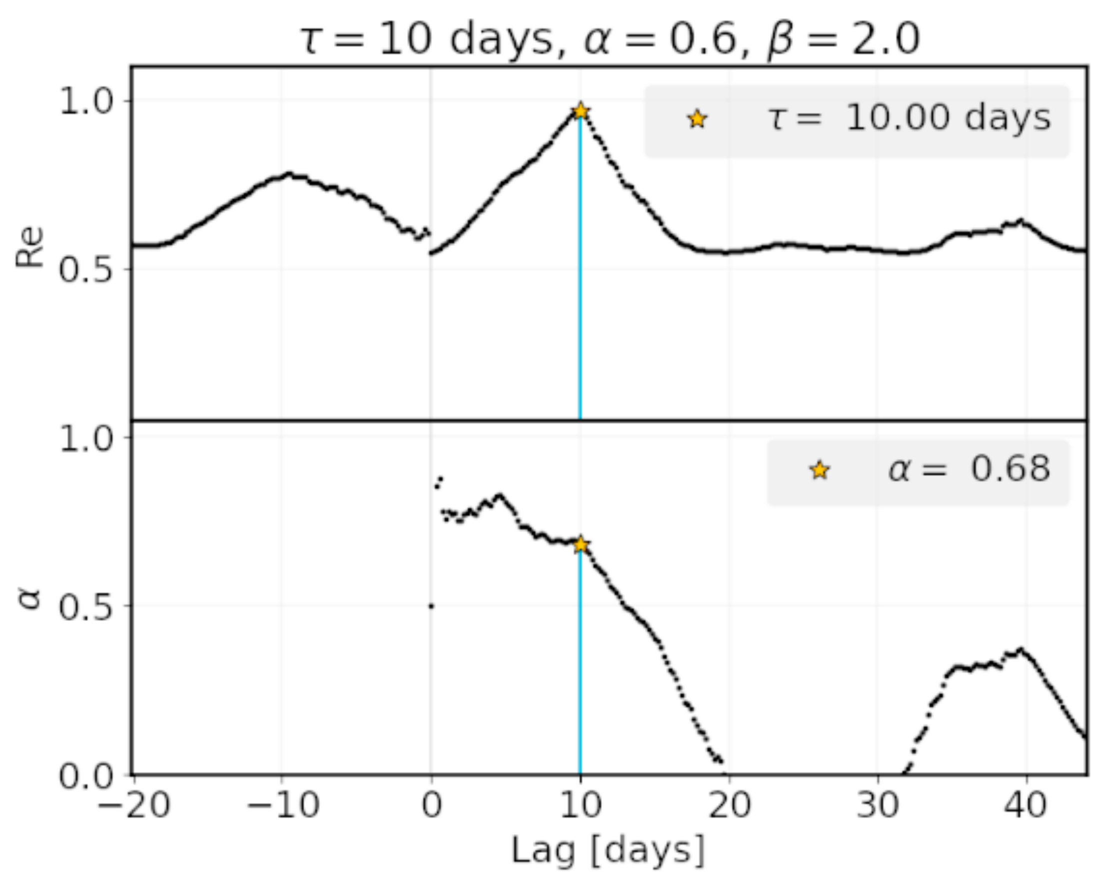

Methods

Time delay determination: τ-α formalism

Simulations and testing:

- Check formalism, compare with correlation methods.
  ICCF(Gaskel&Sparke86), Javelin (Zu+16)

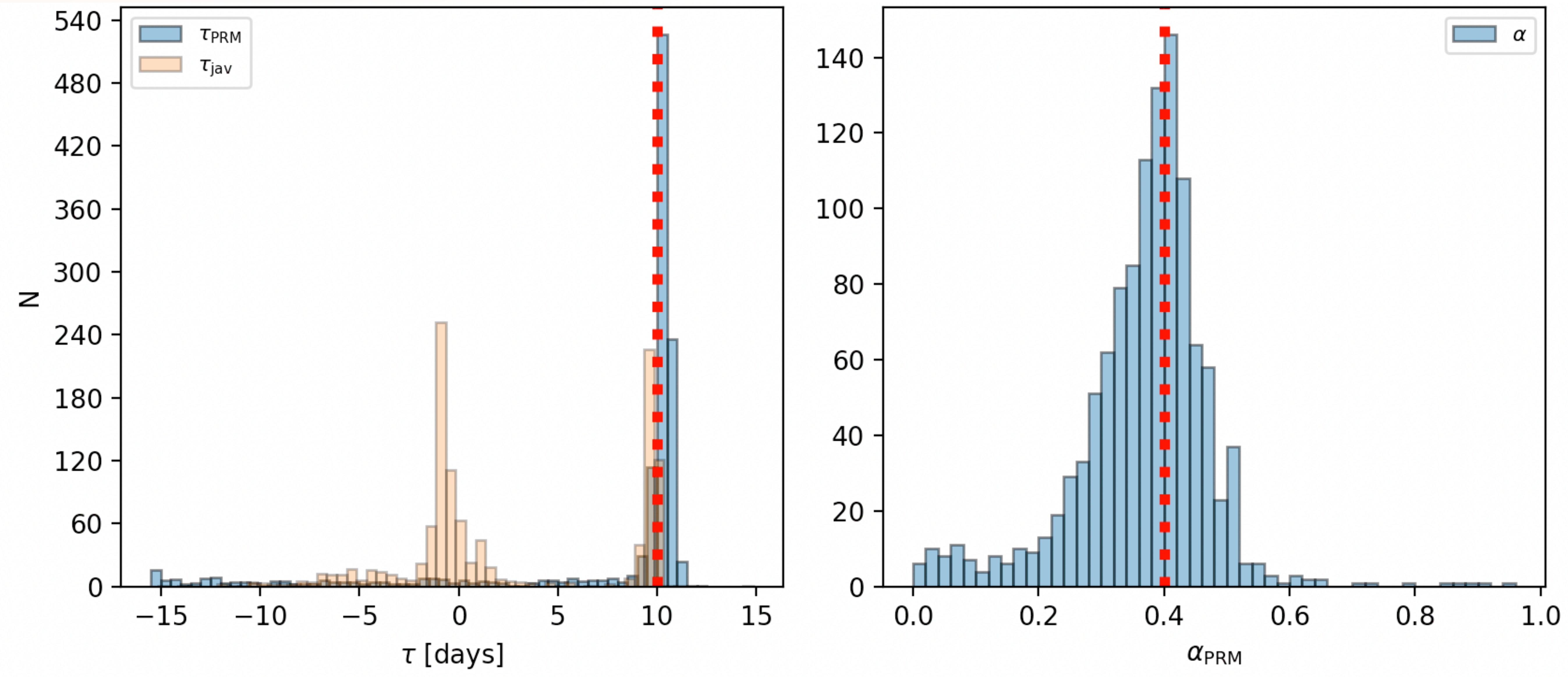

General steps:

- Default limit α between 0.25 and 0.85
- Centroid: weighted average for lag range within $0.8 \times (R_{e,\max} - R_{e,\min})$; analog to the ICCF centroid
- Statistics and Confidence level

Methods

Time delay determination: τ-α formalism

Example formalism for Mrk841, z = 0.036

- Peak/centroid BLR delay $t_{\rm BLR} \sim$ 22 days - Peak/centroid α ~ 0.4 Varying component within the Narrow Band is 40%
- restframe $R_{\rm BLR} = ct_{\rm BLR}/(1+z) \sim$ 21.2 light days

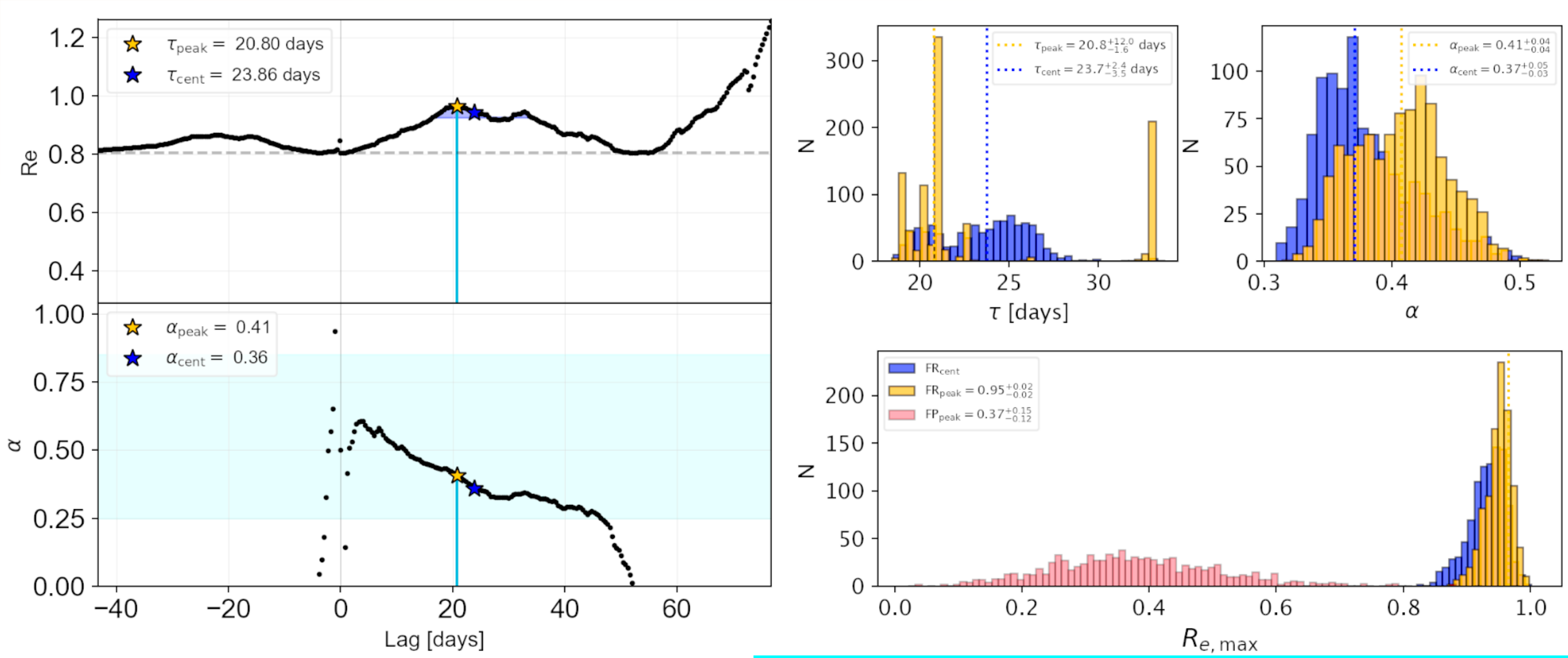

Result: 80% of the sources with Confidence level > 90%

Methods

BH mass estimation

Virial theorem:

relate the BLR's size and the velocity of the gas in the BLR

$$M_{BH} = R_{BLR}\frac{v^2}{G} \sim \langle f \rangle \, ct_{BLR} \frac{FWHM^2_{H\alpha}}{G}$$

$\langle f \rangle$ Depends on AGN geometry. Can vary from 1 - 6

(Grier+13, Graham+11, Park+12)

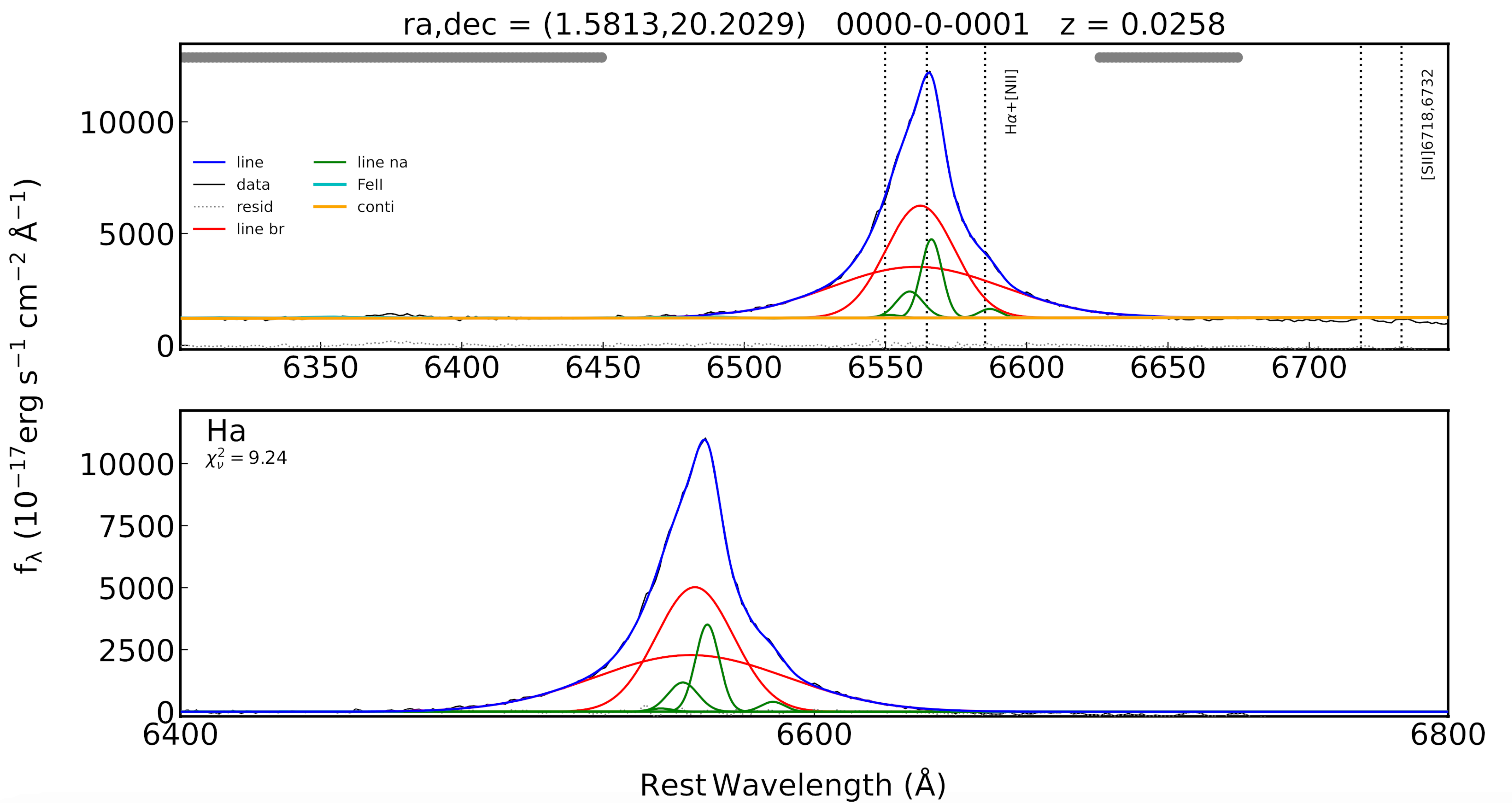

Estimate Hα FWHM:

- Single-epoch spectra:
  - Simultaneously with photometry for 40% of the sources (FAST, SALT)
  - Additional spectra from Literature (6dF, BAT, single studies)
- Procedure:
  - Subtract narrow components [NII] doublet, Hα
  - Broad Hα component: mid + broad or broad
  - Assume $\langle f \rangle$ unity

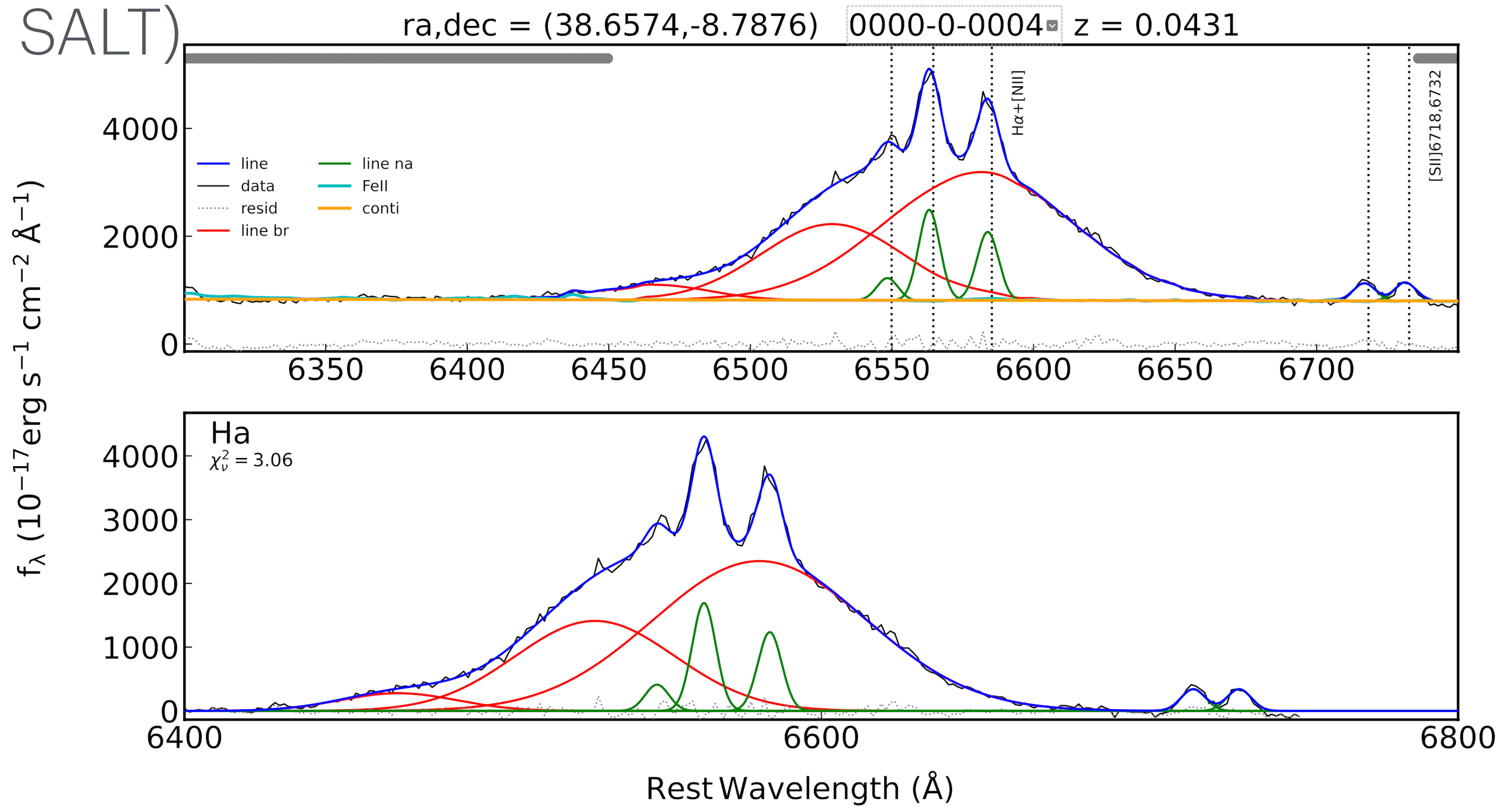

Result: 45 objects BH Mass estimations

Methods

AGN Luminosity and accretion rate estimation

Remove the host galaxy contamination from the AGN:

- Flux Variation Gradient (FVG): AGN vary in time, host remains constant
  Intersection: host component. *(Choloniewski+81,Winkler+92)*
- Check FVG for different epochs: Method to find Changing Look?

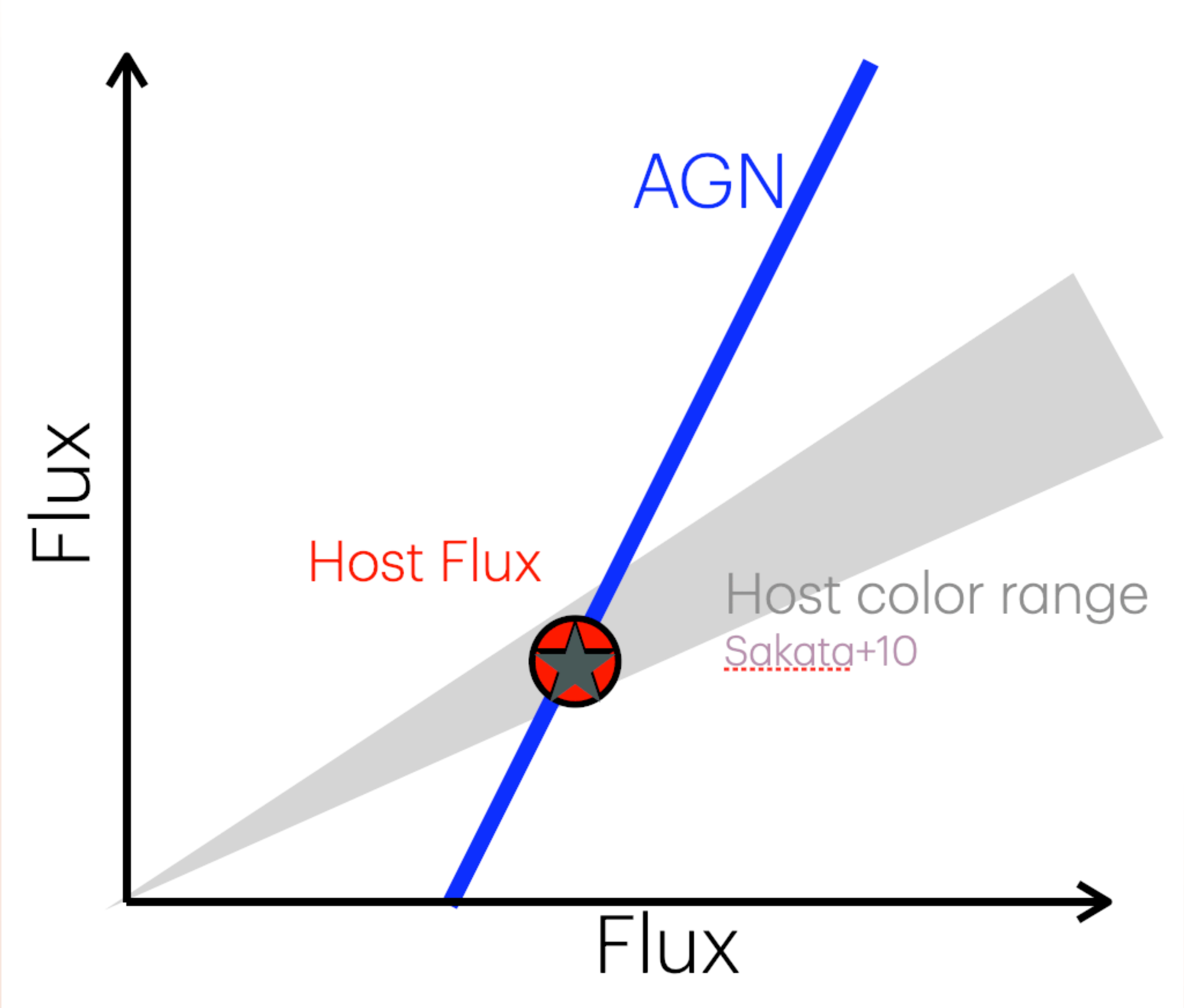

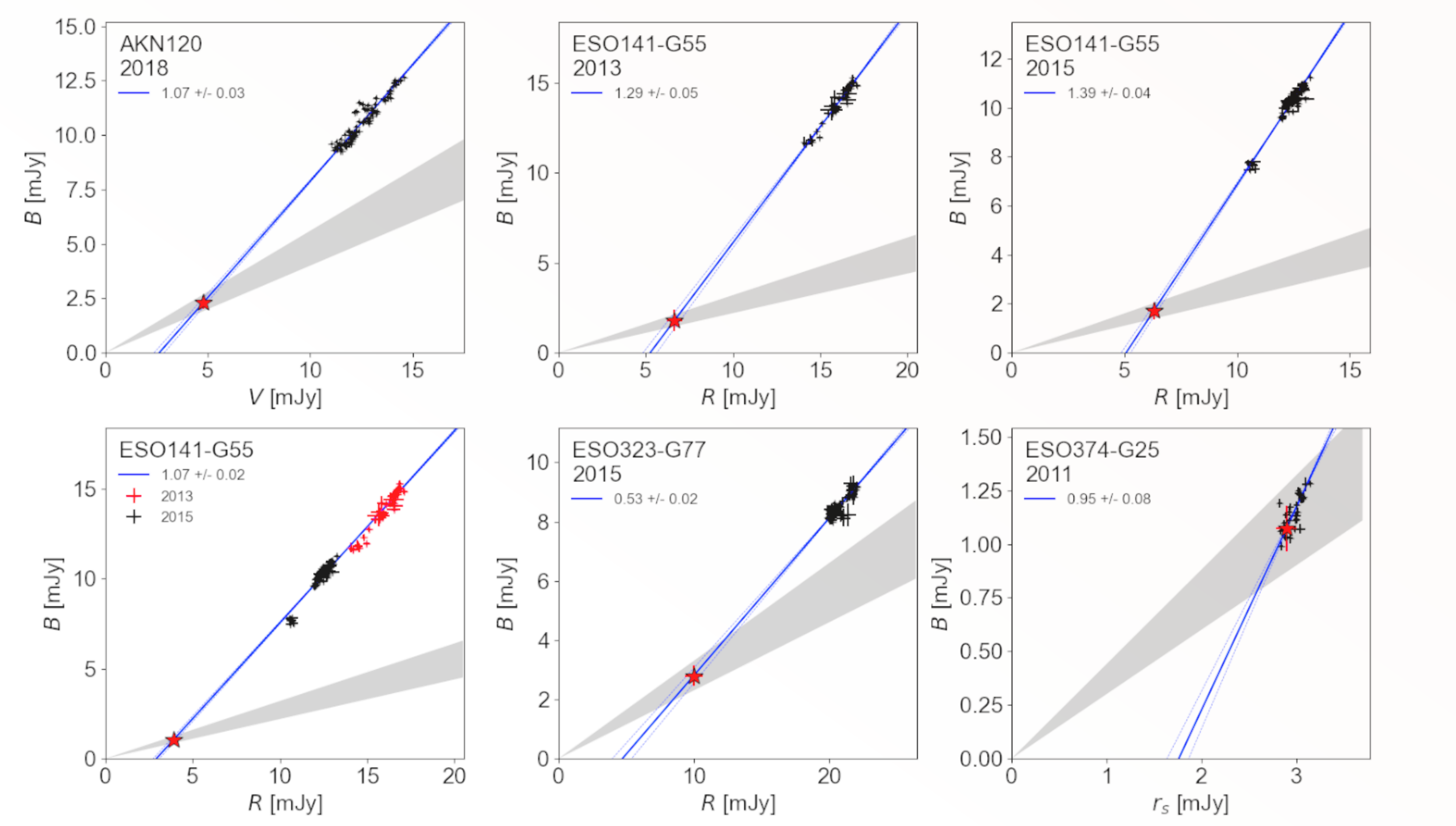

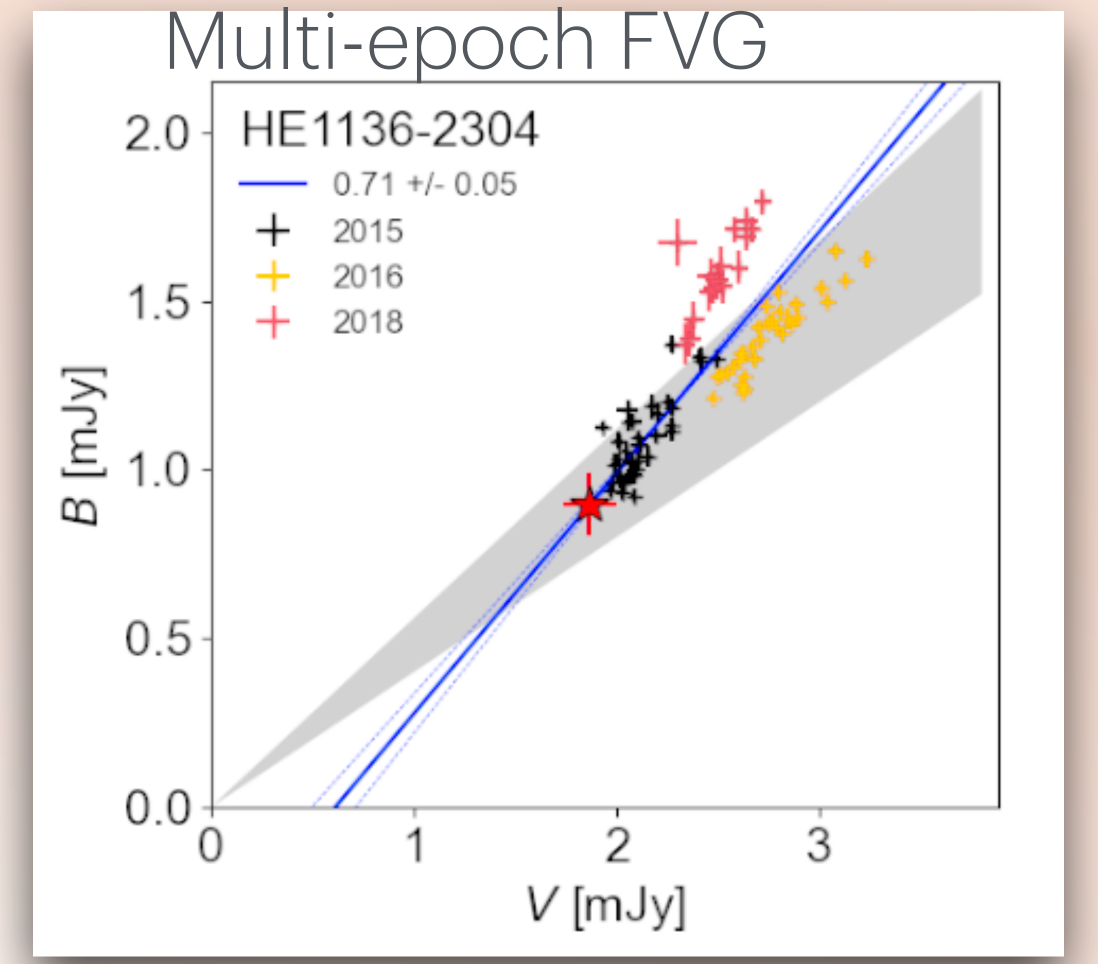

Accretion rate estimation: *(Du+16)*

$$\dot{\mathscr{M}} = 20.1\left(\frac{l_{44}}{cos(\theta)}\right)^{3/2} m_7^{-2}$$

l_{44} = AGN luminosity
m_7 = BH mass
θ = AGN Inclination

Result: host component successfully subtracted in 40 objects
11 High accreting objects

Results

BLR Sizes:

- results for 47 Sources out of the 80 initially
- ~ 80% sources with Confidence level > 90%

40/48 objects ~ 80% successful host subtraction

30 single-epoch BLR sizes and **AGN luminosity**

9 multi-epoch sources

45 objects with **BH mass** estimation

Object	z	Year [days]	$\tau_{\rm cent}$ [days]	F_{5100} [mJy]	L_{5100} [10^{43} erg/s]	FWHM [km/s]	M_{BH} [$10^7 M_\odot$]	$\dot{\mathscr{M}}$
HE0003	0.03345	2014	$6.6^{+1.4}_{-1.7}$	2.24 ± 0.61	3.6 ± 0.99	3396.0 ± 0.0	$1.44^{+0.1}_{-0.12}$	$3.2^{+10.8}_{-10.81}$
WPVS007	0.02861	2012	$10.6^{+0.9}_{-1.0}$	2.19 ± 0.38	2.55 ± 0.45	1557.0 ± 163.0	$0.49^{+0.04}_{-0.05}$	$16.6^{+4.45}_{-4.66}$
IRAS010	0.02392	2013	$38.3^{+4.0}_{-10.7}$	1.93 ± 0.44	1.53 ± 0.34	1731.0 ± 124.0	$2.2^{+0.26}_{-0.68}$	$0.38^{+0.12}_{-0.25}$
NGC985	0.04314	2014	$22.2^{+0.7}_{-0.8}$	3.81 ± 0.84	10.42 ± 0.02	4675.0 ± 347.0	$9.12^{+0.32}_{-0.37}$	$0.4^{+0.03}_{-0.03}$
NGC1019	0.02434	2011	$9.7^{+2.0}_{-0.8}$	0.69 ± 0.09	0.56 ± 0.07	2755.0 ± 80.0	$1.41^{+0.28}_{-0.11}$	$0.21^{+0.09}_{-0.05}$
3C120	0.03301	2014	$57.1^{+5.9}_{-5.9}$	8.95 ± 0.64	14.4 ± 1.05	2924.0 ± 66.0	$9.27^{+0.96}_{-0.96}$	$0.62^{+0.14}_{-0.14}$
AKN120	0.0327	2018	$28.1^{+1.4}_{-1.6}$	7.48 ± 0.28	11.9 ± 0.5	5759.0 ± 12.0	$17.7^{+0.6}_{-0.69}$	$0.13^{+0.02}_{-0.02}$
RXSJ062	0.03778	2013	$19.5^{+0.2}_{-1.4}$	1.25 ± 0.21	2.76 ± 0.46	1506.0 ± 30.0	$0.84^{+0.01}_{-0.06}$	$6.42^{+1.15}_{-1.51}$
MRK705	0.02879	2013	$15.5^{+1.0}_{-0.7}$	1.97 ± 0.18	2.61 ± 0.24	1919.0 ± 332.0	$1.09^{+0.05}_{-0.04}$	$3.49^{+0.73}_{-0.69}$
IRAS095	0.055	2013	$21.4^{+2.5}_{-2.1}$	0.51 ± 0.15	2.32 ± 0.25	2402.0 ± 18.0	$2.3^{+0.29}_{-0.24}$	$0.66^{+0.18}_{-0.16}$
HE1143	0.03295	2016	$17.5^{+2.5}_{-2.4}$	2.88 ± 0.24	5.03 ± 0.41	2143.0 ± 15.0	$1.53^{+0.27}_{-0.26}$	$4.74^{+1.72}_{-1.65}$
ESO323	0.01501	2015	$26.7^{+3.6}_{-1.9}$	4.45 ± 0.17	1.61 ± 0.06	4246.0 ± 460.0	$9.3^{+1.39}_{-0.73}$	$0.02^{+0.01}_{-0.0}$
MRK1347	0.04995	2014	$13.8^{+4.6}_{-1.7}$	1.6 ± 0.28	6.48 ± 1.16	1576.0 ± 540.0	$0.64^{+0.34}_{-0.13}$	$39.38^{+42.48}_{-16.01}$
ESO578	0.03502	2014	$19.5^{+0.6}_{-0.6}$	1.41 ± 0.17	2.73 ± 0.28	5125.0 ± 14.0	$9.7^{+0.31}_{-0.31}$	$0.05^{+0.01}_{-0.01}$
MRK841	0.03642	2014	$23.8^{+2.5}_{-2.4}$	3.33 ± 0.18	6.87 ± 0.38	4645.0 ± 734.0	$9.72^{+0.92}_{-0.89}$	$0.19^{+0.04}_{-0.04}$
NGC5940	0.03408	2014	$5.9^{+0.8}_{-0.7}$	0.95 ± 0.14	1.71 ± 0.26	4033.0 ± 22.0	$1.82^{+0.22}_{-0.2}$	$0.66^{+0.22}_{-0.2}$
MCG+03	0.04	2013	$16.8^{+0.4}_{-0.5}$	0.28 ± 0.22	0.6 ± 0.5			
CTSG03	0.04002	2013	$17.8^{+0.9}_{-0.9}$	1.04 ± 0.17	2.49 ± 0.41	3042.0 ± 242.0	$3.11^{+0.14}_{-0.14}$	$0.4^{+0.11}_{-0.11}$
ESO399	0.025	2011	$19.6^{+0.4}_{-0.8}$	2.47 ± 0.34	2.1 ± 0.3	1843.0 ± 81.0	$1.27^{+0.03}_{-0.07}$	$1.84^{+0.21}_{-0.27}$
NGC6860	0.01488	2015	$34.7^{+1.0}_{-1.1}$	2.0 ± 0.49	0.61 ± 0.15	3668.0 ± 1016.0	$9.02^{+0.27}_{-0.3}$	$0.01^{+0.0}_{-0.0}$
MRK509	0.0344	2014	$22.9^{+0.8}_{-0.8}$	7.23 ± 2.38	14.23 ± 0.4	3451.0 ± 32.0	$5.17^{+0.2}_{-0.2}$	$1.96^{+0.16}_{-0.16}$
1H2107	0.02698	2012	$12.1^{+3.3}_{-0.6}$	4.81 ± 0.12	4.76 ± 0.12	2333.0 ± 447.0	$1.26^{+0.23}_{-0.04}$	$6.43^{+2.42}_{-0.6}$
HE2128	0.05248	2016	$8.3^{+0.7}_{-0.9}$	0.59 ± 0.05	2.43 ± 0.2	1660.0 ± 124.0	$0.43^{+0.04}_{-0.05}$	$20.41^{+4.3}_{-5.39}$
NGC7214	0.02385	2011	$6.9^{+5.2}_{-0.9}$	2.73 ± 0.53	2.08 ± 0.41	3662.0 ± 100.0	$1.77^{+1.03}_{-0.18}$	$0.93^{+1.15}_{-0.41}$
UGC1213	0.02509	2012	$15.0^{+0.5}_{-0.4}$	2.06 ± 0.49	1.7 ± 0.4	2693.0 ± 269.0	$2.08^{+0.08}_{-0.06}$	$0.5^{+0.12}_{-0.11}$
NGC7469	0.01627	2012	$9.6^{+3.5}_{-4.8}$	9.66 ± 0.96	3.12 ± 0.31	1615.0 ± 119.0	$0.48^{+0.3}_{-0.41}$	$23.1^{+28.54}_{-39.14}$
F1041	0.03347	2013	$15.7^{+0.7}_{-1.0}$	0.65 ± 0.19	1.03 ± 0.3	3676.0 ± 886.0	$4.03^{+0.19}_{-0.28}$	$0.06^{+0.02}_{-0.02}$
NGC7603	0.02876	2014	$35.1^{+1.5}_{-1.3}$	7.16 ± 0.99	7.98 ± 1.1	5778.0 ± 10.0	$22.34^{+1.03}_{-0.89}$	$0.04^{+0.01}_{-0.01}$
IRAS232	0.0359	2013	$13.9^{+5.2}_{-5.7}$	2.14 ± 0.43	3.94 ± 0.79			
UM163	0.03343	2013	$10.9^{+0.4}_{-0.5}$	1.37 ± 0.2	2.13 ± 0.31	4901.0 ± 77.0	$4.97^{+0.17}_{-0.22}$	$0.12^{+0.03}_{-0.03}$

MRK335	0.02578	2010	$19.0^{+0.4}_{-0.3}$		3.13 ± 0.36	1611.0 ± 259.0	$0.94^{+0.02}_{-0.02}$	$6.1^{+0.79}_{-0.77}$
MRK335	0.02578	2011	$17.5^{+3.9}_{-6.6}$	5.51 ± 0.2	4.9 ± 0.17	1611.0 ± 259.0	$0.87^{+0.23}_{-0.39}$	$14.08^{+7.51}_{-12.7}$
MRK335	0.02578	2014	$12.0^{+0.9}_{-1.1}$	4.87 ± 0.25	4.34 ± 0.23	1611.0 ± 259.0	$0.6^{+0.04}_{-0.05}$	$24.96^{+3.97}_{-4.7}$
WPVS48	0.037	2013	$21.1^{+0.9}_{-1.9}$	2.69 ± 0.2	5.66 ± 0.42	1917.0 ± 24.0	$1.47^{+0.05}_{-0.11}$	$6.13^{+0.86}_{-1.2}$
WPVS48	0.037	2014	$18.3^{+0.6}_{-1.3}$	2.69 ± 0.54	5.66 ± 1.13	1917.0 ± 24.0	$1.27^{+0.04}_{-0.08}$	$8.15^{+2.33}_{-2.52}$
WPVS48	0.037	2018	$19.3^{+4.3}_{-0.3}$	2.29 ± 0.4	4.82 ± 0.84	1917.0 ± 24.0	$1.34^{+0.31}_{-0.02}$	$5.76^{+2.91}_{-1.11}$
ESO438	0.02401	2011	$10.8^{+0.6}_{-1.6}$	3.94 ± 0.74	3.64 ± 0.68	2300.0 ± 167.0	$1.09^{+0.09}_{-0.23}$	$5.68^{+1.09}_{-2.44}$
ESO438	0.02401	2015	$7.7^{+0.8}_{-0.6}$	2.92 ± 0.3	2.68 ± 0.27	2300.0 ± 167.0	$0.78^{+0.13}_{-0.1}$	$7.06^{+2.44}_{-1.84}$
HE1136	0.027	2015	$9.1^{+0.5}_{-0.2}$	0.19 ± 0.12	0.22 ± 0.14	3544.0 ± 221.0	$2.18^{+0.14}_{-0.06}$	$0.02^{+0.01}_{-0.01}$
HE1136	0.027	2016	$17.4^{+2.2}_{-3.9}$	0.74 ± 0.12	0.84 ± 0.14	3544.0 ± 221.0	$4.17^{+0.64}_{-1.13}$	$0.04^{+0.01}_{-0.02}$
HE1136	0.027	2018	$11.2^{+4.2}_{-1.8}$	0.66 ± 0.12	0.75 ± 0.14	3544.0 ± 221.0	$2.69^{+1.02}_{-0.44}$	$0.09^{+0.07}_{-0.03}$
PGC5024	0.02346	2011	$21.6^{+0.9}_{-0.9}$	1.08 ± 0.12	0.93 ± 0.11	2377.0 ± 11.0	$2.34^{+0.1}_{-0.1}$	$0.16^{+0.03}_{-0.03}$
PGC5024	0.02346	2014	$14.2^{+1.0}_{-0.9}$	1.49 ± 0.16	1.28 ± 0.13	2377.0 ± 11.0	$1.54^{+0.09}_{-0.08}$	$0.6^{+0.13}_{-0.13}$
ESO511	0.02239	2013	$20.9^{+0.7}_{-0.5}$	1.28 ± 0.32	0.99 ± 0.02	3656.0 ± 12.0	$5.36^{+0.15}_{-0.11}$	$0.03^{+0.0}_{-0.0}$
ESO511	0.02239	2014	$19.2^{+0.5}_{-0.6}$	0.71 ± 0.05	0.55 ± 0.04	3656.0 ± 12.0	$4.92^{+0.13}_{-0.15}$	$0.02^{+0.0}_{-0.0}$
RXSJ174	0.023	2012	$19.8^{+0.5}_{-0.5}$	3.16 ± 0.27	2.14 ± 0.21	2222.0 ± 129.0	$1.87^{+0.04}_{-0.04}$	$0.87^{+0.15}_{-0.15}$
RXSJ174	0.023	2014	$23.1^{+5.2}_{-1.2}$	3.21 ± 0.6	2.45 ± 0.46	2222.0 ± 129.0	$2.19^{+0.62}_{-0.14}$	$0.79^{+0.46}_{-0.15}$
ESO141	0.03711	2013	$19.5^{+0.7}_{-0.5}$	12.21 ± 0.84	25.1 ± 1.7	4981.0 ± 578.0	$9.15^{+0.18}_{-0.13}$	$1.47^{+0.4}_{-0.4}$
ESO141	0.03711	2015	$22.2^{+0.2}_{-0.2}$	8.6 ± 0.57	17.2 ± 2.0	4981.0 ± 578.0	$10.42^{+0.11}_{-0.11}$	$0.64^{+0.07}_{-0.07}$
PGC6498	0.01937	2013	$27.6^{+2.3}_{-3.7}$	0.9 ± 0.04	0.45 ± 0.02	3275.0 ± 770.0	$5.7^{+0.43}_{-0.69}$	$0.01^{+0.0}_{-0.0}$
PGC6498	0.01937	2014	$26.0^{+0.3}_{-0.3}$	1.05 ± 0.04	0.52 ± 0.02	3275.0 ± 770.0	$5.37^{+0.07}_{-0.07}$	$0.01^{+0.0}_{-0.0}$

ESO549	0.02627	2012	$7.0^{+5.6}_{-1.3}$	< 4.73	< 1.11	2766.0 ± 270.0	$1.02^{+0.91}_{-0.21}$	< 9.07
MCG0212	0.036	2014	$10.8^{+1.3}_{-1.2}$	< 2.31	< 5.67	5585.0 ± 782.0	$6.38^{+0.71}_{-0.65}$	< 0.22
ESO490	0.02485	2011	$13.0^{+4.5}_{-2.7}$	< 3.98	< 9.08	5588.0 ± 412.0	$7.77^{+3.22}_{-1.93}$	< 0.11
MRK1239	0.01993	2015	$24.4^{+22.0}_{-7.1}$	< 5.51	< 0.55	1043.0 ± 358.0	$0.51^{+0.5}_{-0.16}$	< 24.28
ESO374	0.02367	2011	$11.2^{+1.0}_{-2.0}$	< 1.83	< 2.92	4481.0 ± 969.0	$4.31^{+0.27}_{-0.53}$	< 0.1
PG1149	0.049	2013	$17.3^{+6.2}_{-1.1}$	< 1.4	< 5.36	3579.0 ± 700.0	$4.14^{+2.02}_{-0.36}$	< 0.68
NGC4726	0.0245	2013	$16.6^{+0.7}_{-1.0}$	< 3.01	< 3.24	3119.0 ± 0.0	$3.09^{+0.14}_{-0.2}$	< 0.55
IC4329A	0.01605	2015	$22.7^{+0.8}_{-0.8}$	< 7.09	< 6.31	4940.0 ± 274.0	$10.69^{+0.23}_{-0.23}$	< 0.04

Radius — Luminosity Relation

Main results

Diferent literature Hα samples

- 14 High luminosity QSO (0.08 < z < 0.3): Kaspi'00
- 7 sources Nearby Seyferts (z ~0.01): Bentz'10
- 23 SDSS sources high redshifted (0.1 < z < 0.45): Shen'23, revised version from Grier'17
- 5 sources (redshifts 0.07 < z < 0.2) Seoul Cho'23
- New sources: 37 Seyferts (0.01 < z < 0.05)
  28 single-epoch and 9 multi-epoch

Scatter:

- All Hα studies = 0.32dex
- SDSS = 0.34dex, This work = 0.28dex
- Compite with big telescopes

Previous studies on broad emission lines:

- Hβ (~120 sources, Bentz+13, Du+16, MAl+19)
- MgII (~30-40 sources Czerny+19, Yu+22)
- CIV (~30-40 sources Lira+18, Kaspi+22)

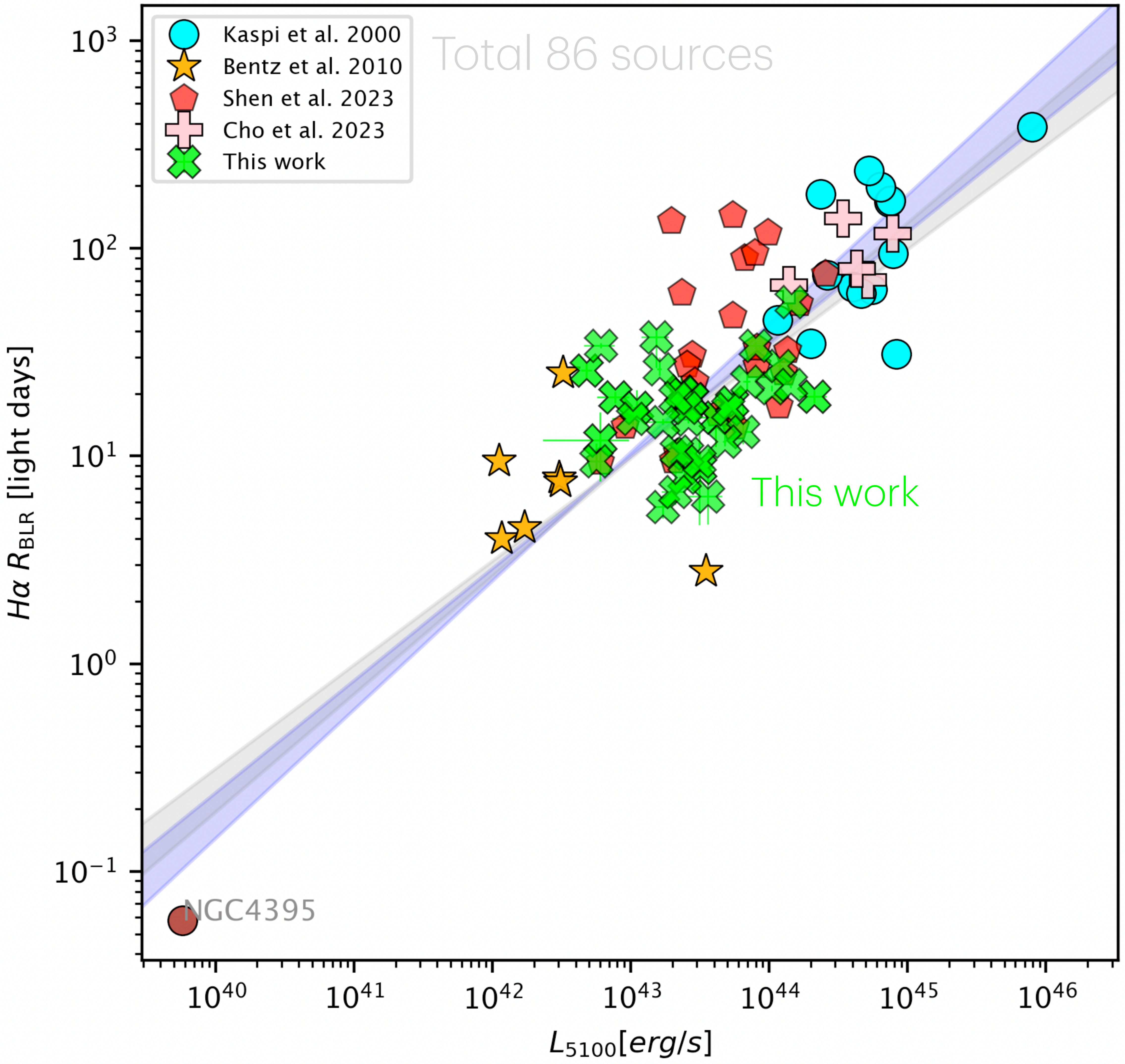

Result: Add a total of 37 Sources in Hα with scatter of 0.28dex

Radius — Luminosity Relation

Multi-epoch observations

<u>Different observations epochs</u>

- Different lag/luminosity at different observing seasons
- Stable results for 6 objects with scatter < 0.07dex
- Comparing with the overall scatter (~0.3dex), single scatter does not affect much (~0.1dex)
- No intrinsic relation found:
    - 3 objects follow slope ~0.5
    - Other objects: random or stable
- Multi-epoch sample not large enough to lead to robust conclusions
- Objects tend to lie within a range of the relation, so that the overall r-L relation and its scatter is not only due to uncertainties in the BLR size or the luminosity

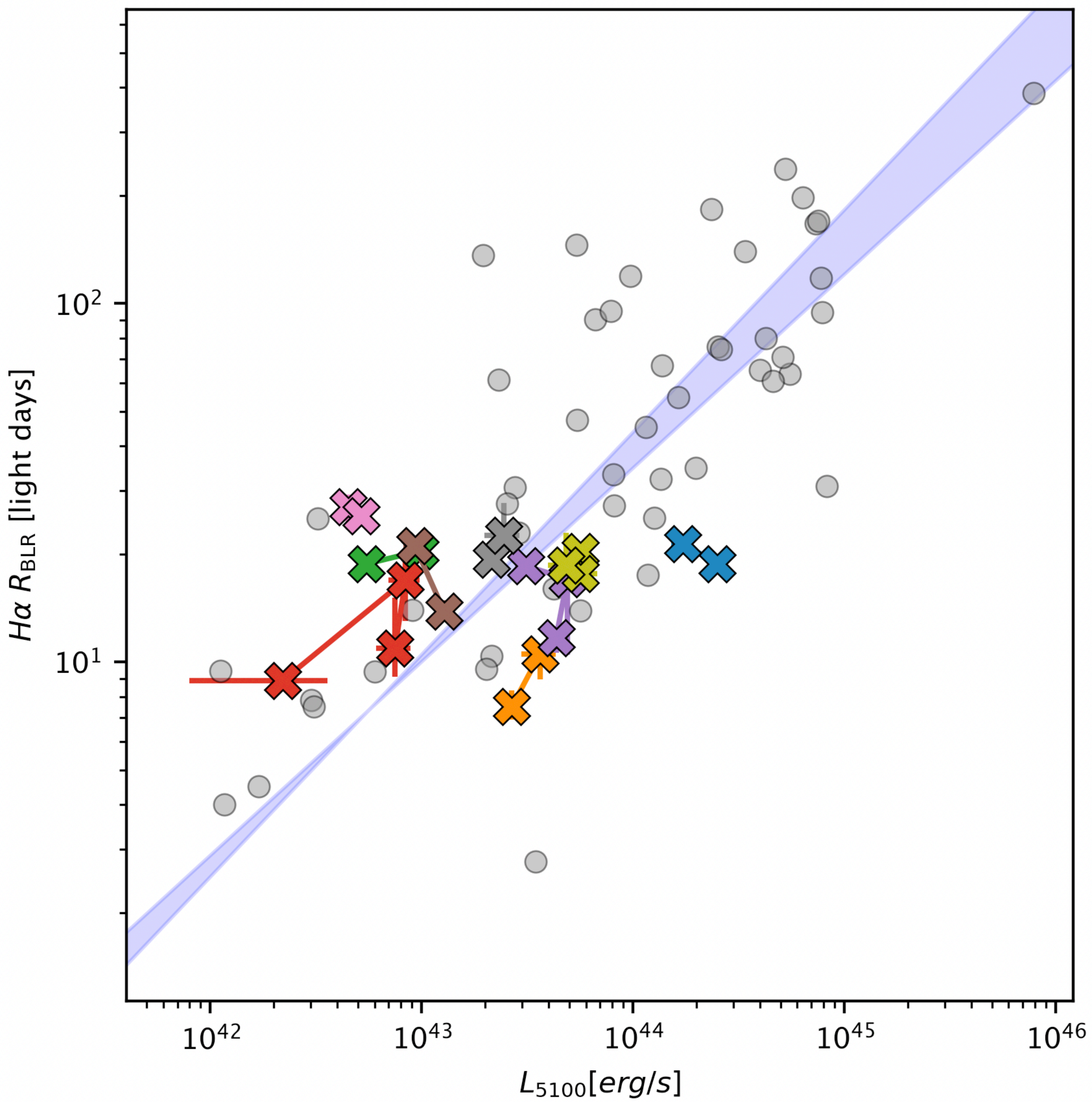

Radius — Luminosity Relation

Accretion rate dependence

$$\dot{\mathscr{M}} = 20.1 \left(\frac{l_{44}}{cos(\theta)} \right)^{3/2} m_7^{-2}$$

<u>Accretion rate dependence is biased by definition:</u>

- More luminous objects move to the right hand, leading to be underneath the sample
- BH mass depends on time delay. If time delay is shorter, accretion rate is higher and high accreting objects stay underneath the sample

- Offset High accreting objects: μ ~ -0.14 with scatter of 0.30dex

<u>Ongoing</u>: evaluate independently the accretion rate

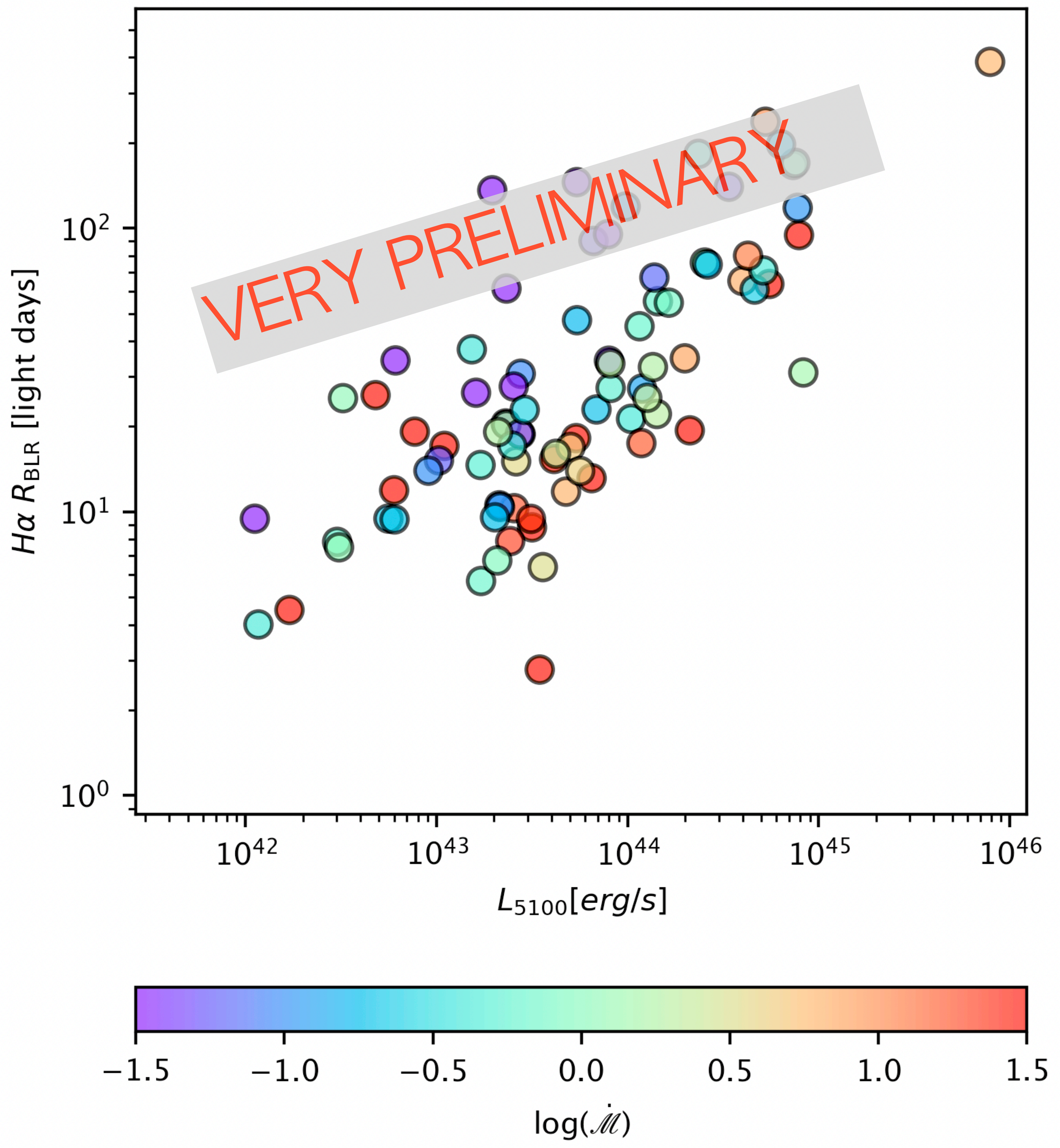

Radius - Luminosity Relation

Summary

- Add a total of 37 sources to the previous Hα RM results
- Large scatter ~0.28dex, but smaller than previous SDSS results ~0.32dex
- Estimate dependence with dimensionless accretion rate
- Hα emission line helpful for investigating origin of the r-L scatter

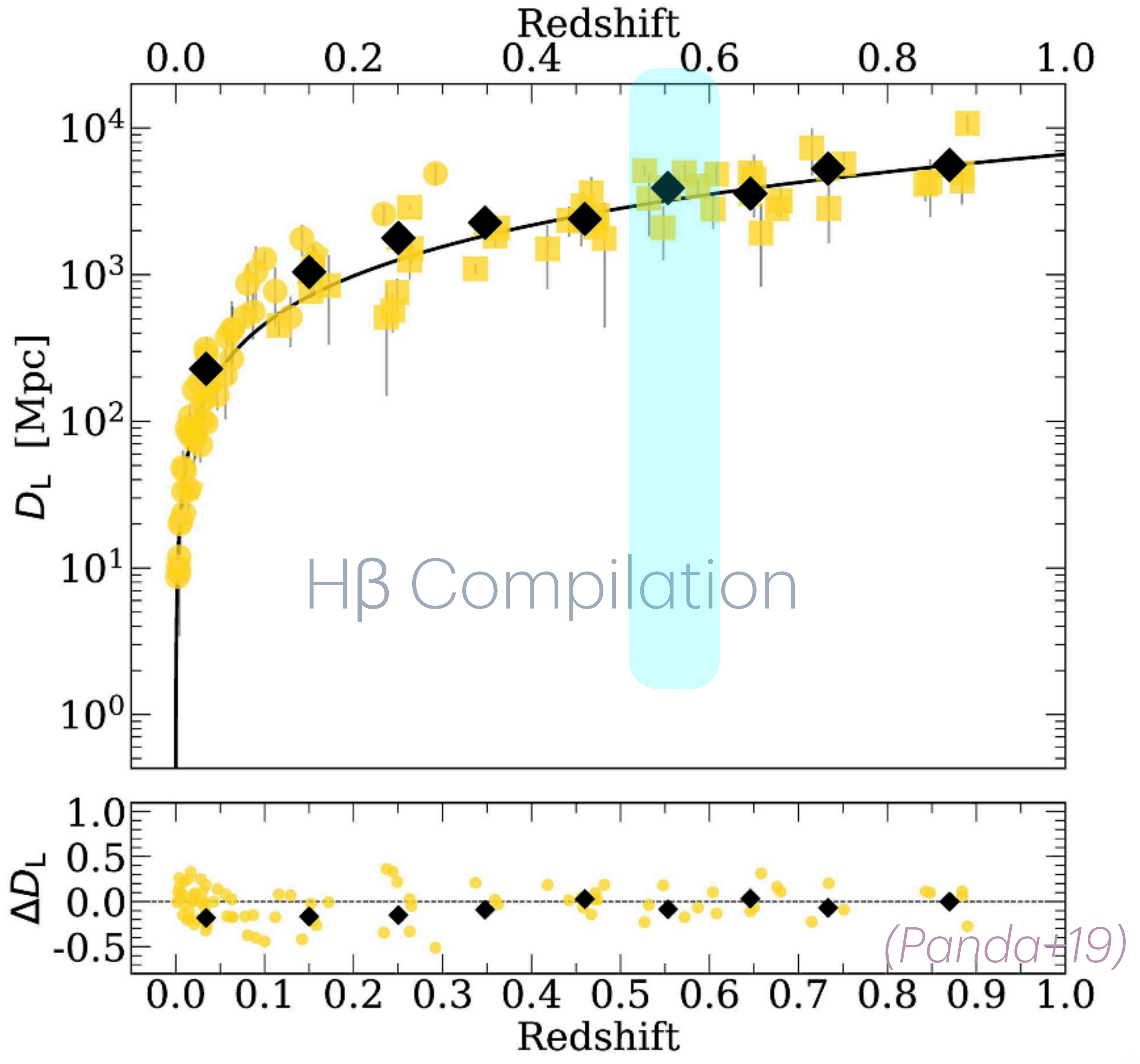

<u>Hα emission line for cosmological purposes</u>

- Advantages:
  - bright, prominent line
  - easier to observe in PRM with small telescopes and Narrow Bands
  - Upcoming LSST survey will observe Hα within Broad bands: z, y
  - Helpful to reduce scatter in the r-L relation
- Disadvantages:
  - Optical regime: Hα possible observations up to redshift z~0.5-0.6, where Hβ (z~1), MgII (z~2.5), CIV (z~5)
  - Expected larger delays, needed longer observations

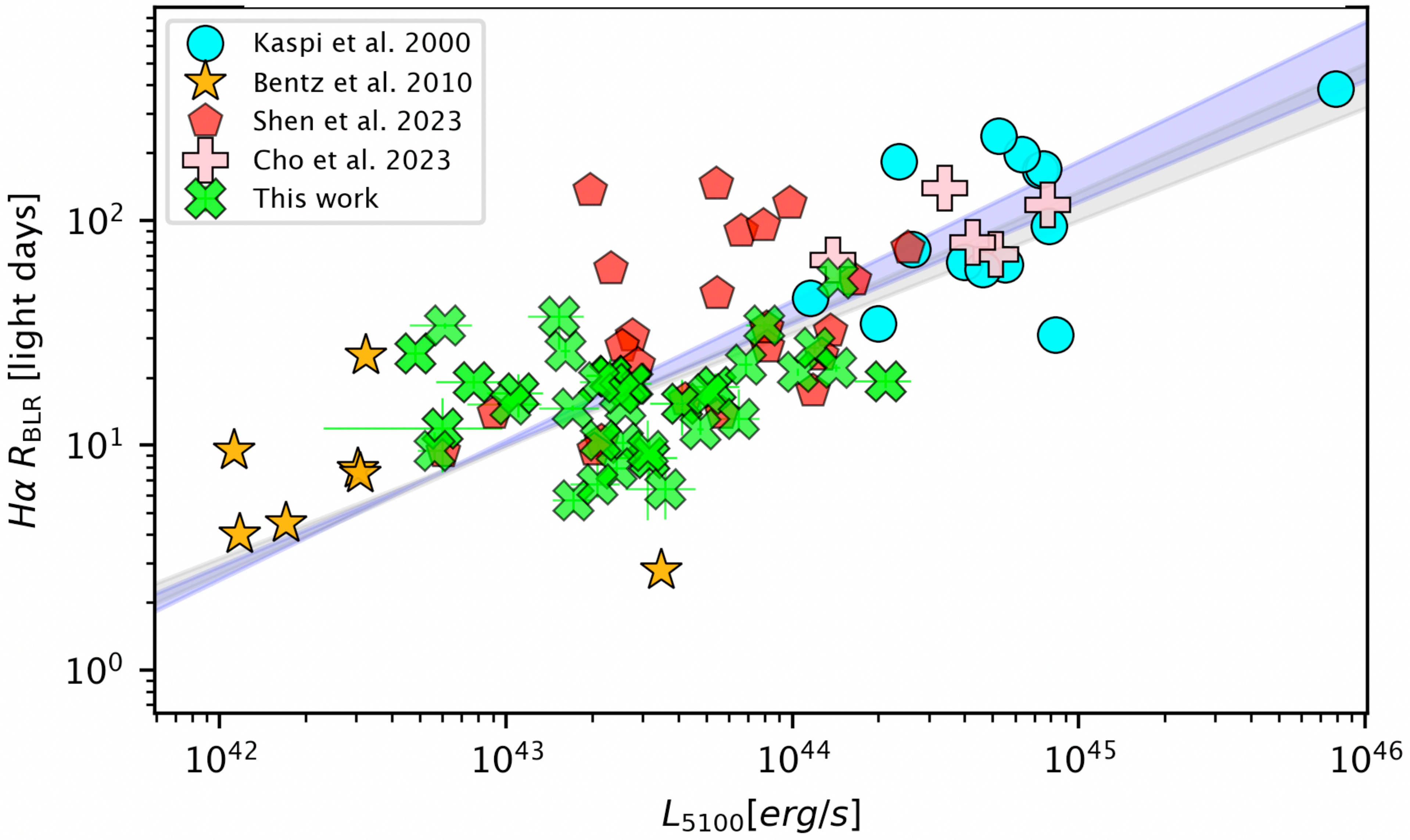

Summary

- Small telescopes (~25cm): provide good data quality and good cadence to explore AGN and the r-L relation for Hα
- Photometric Reverberation mapping technique helps to improve the AGN time delays found with spectroscopic techniques
- Present a new formalism, an easy method for determining time-delays in the PRM context which will help for upcoming surveys, such as LSST
- The exploration of the Flux-Flux diagrams to find Changing look candidates in new surveys
- Hα emission line suitable for exploring the origin of the r-L scatter
  - Advantage: bright line, easier to observe in PRM with small telescopes and Narrow bands.
    - Helpful to check origin of the scatter in the r-L relation
    - Homogeneous sample
  - Disadvantage: optical observations up to redshift 0.5-0.6

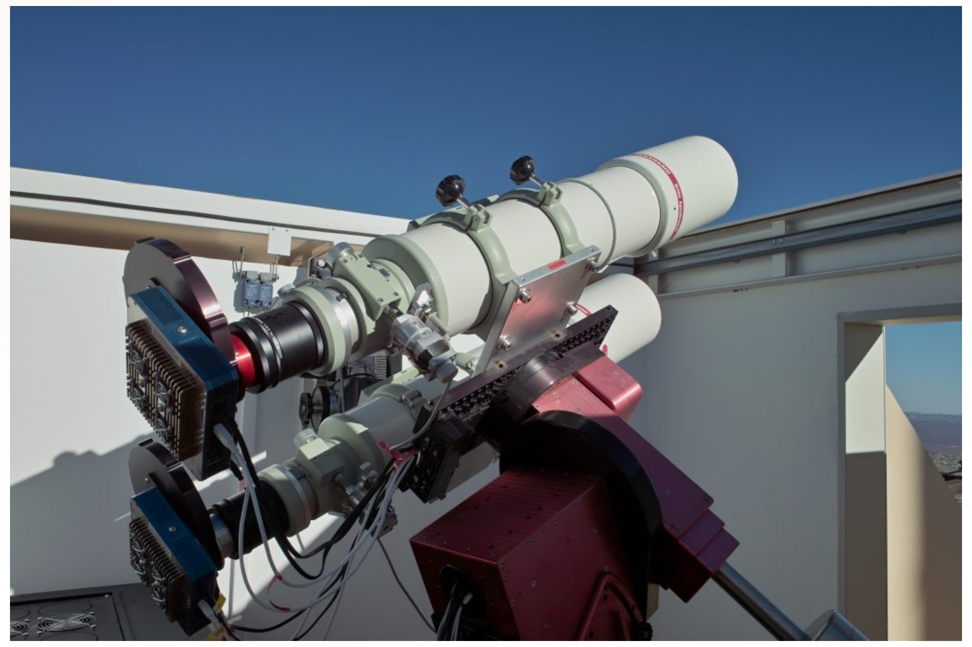

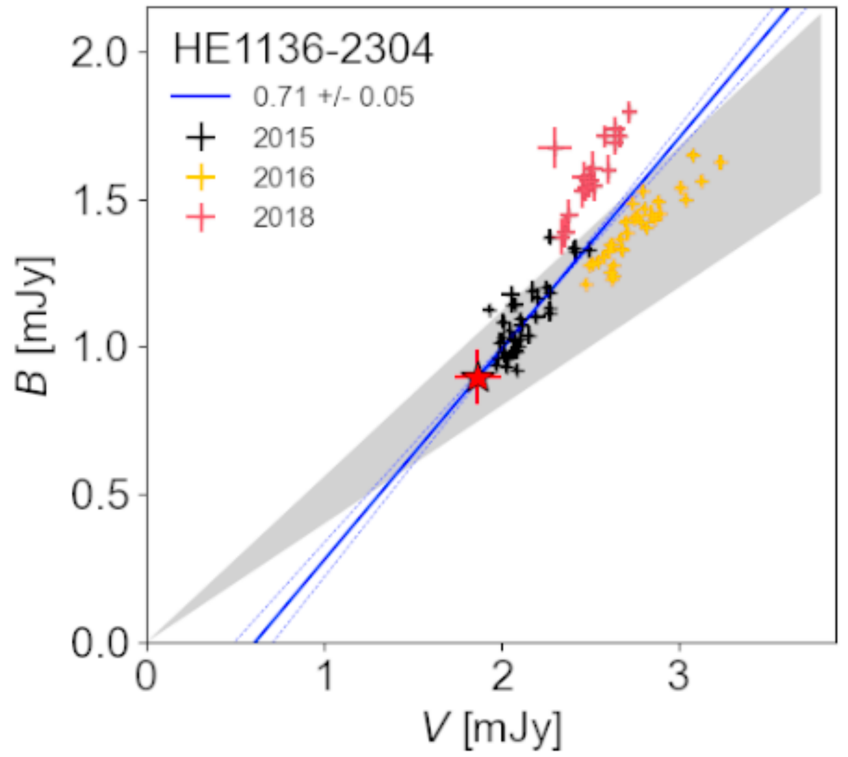

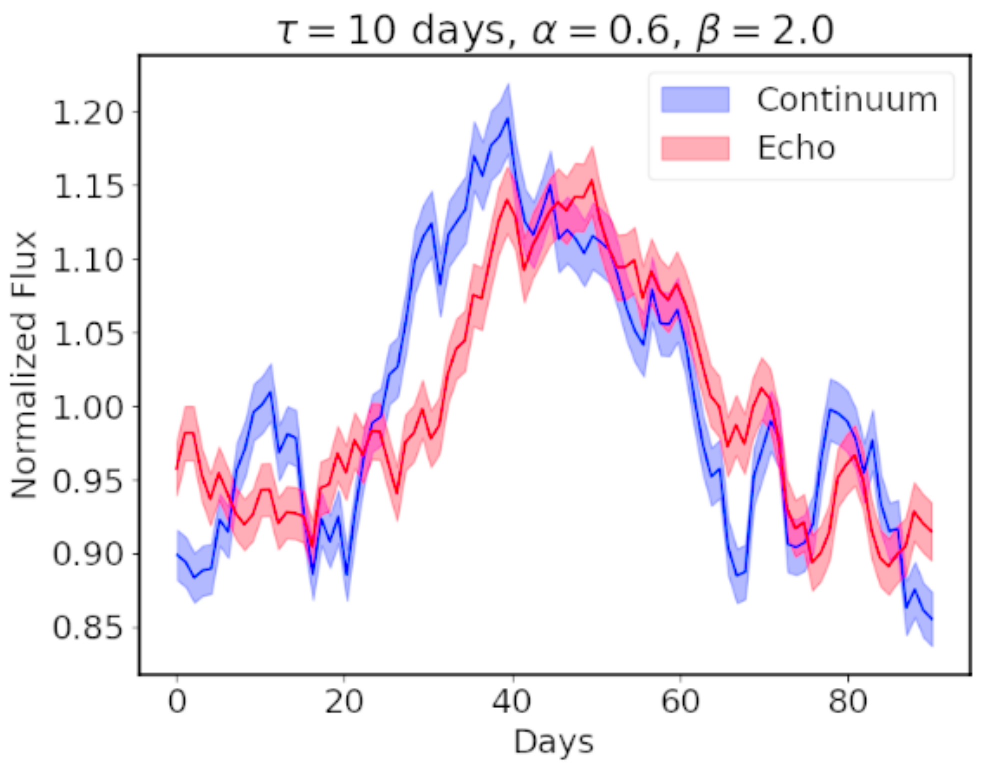

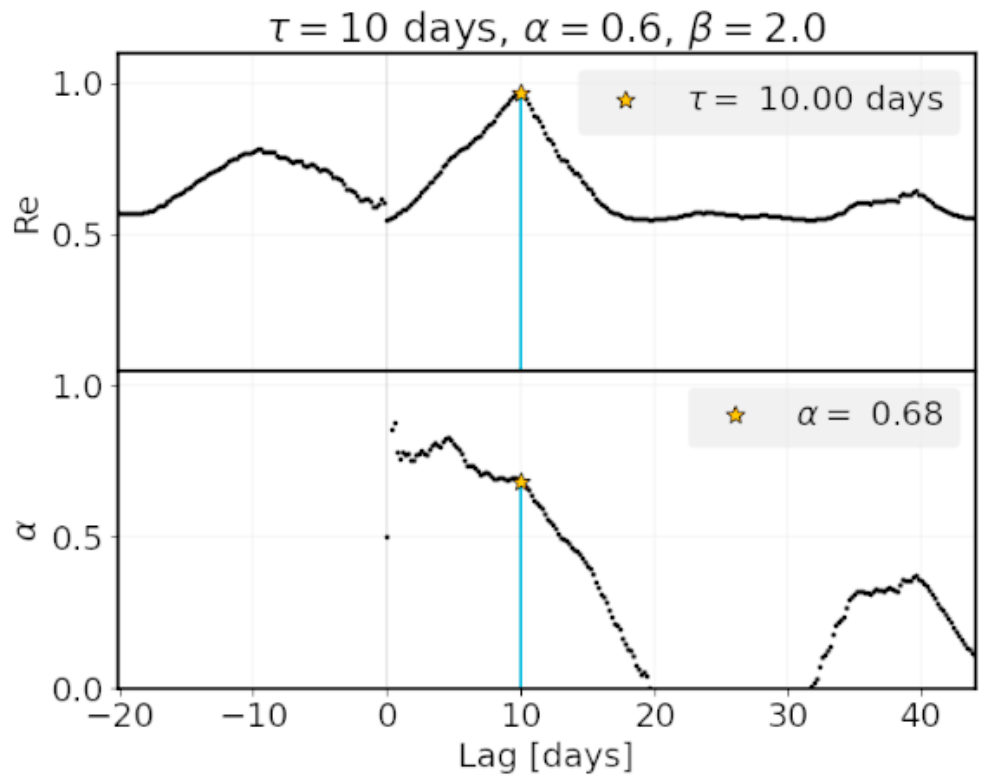

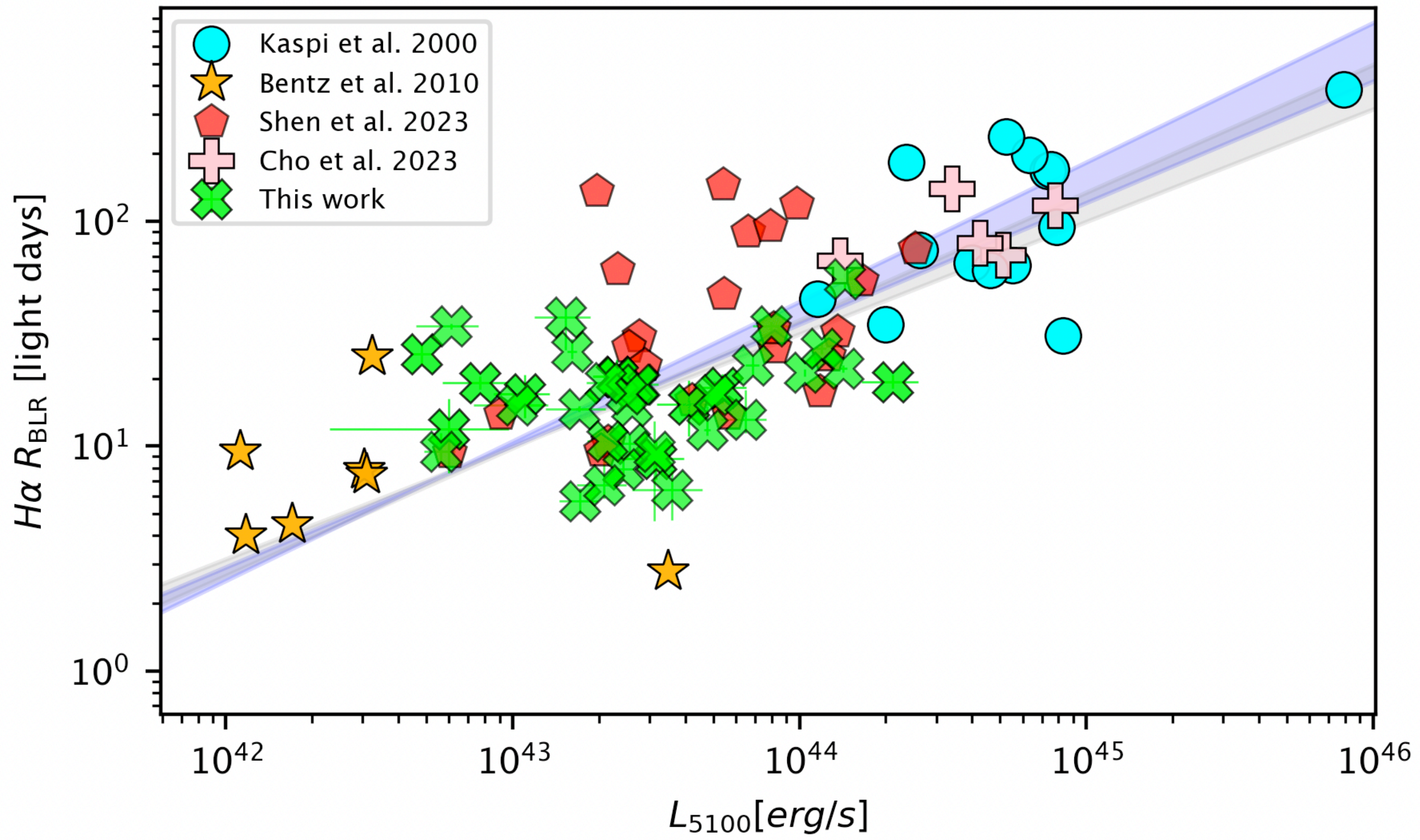

Thank you!

Radius — Luminosity Relation

- Uncertainties: time delay determination and real BLR size, BH mass (unknown AGN geometry)
- Uncertainties: AGN luminosity (removing host component), extinction within AGN
- All produce uncertainties in Accretion rate

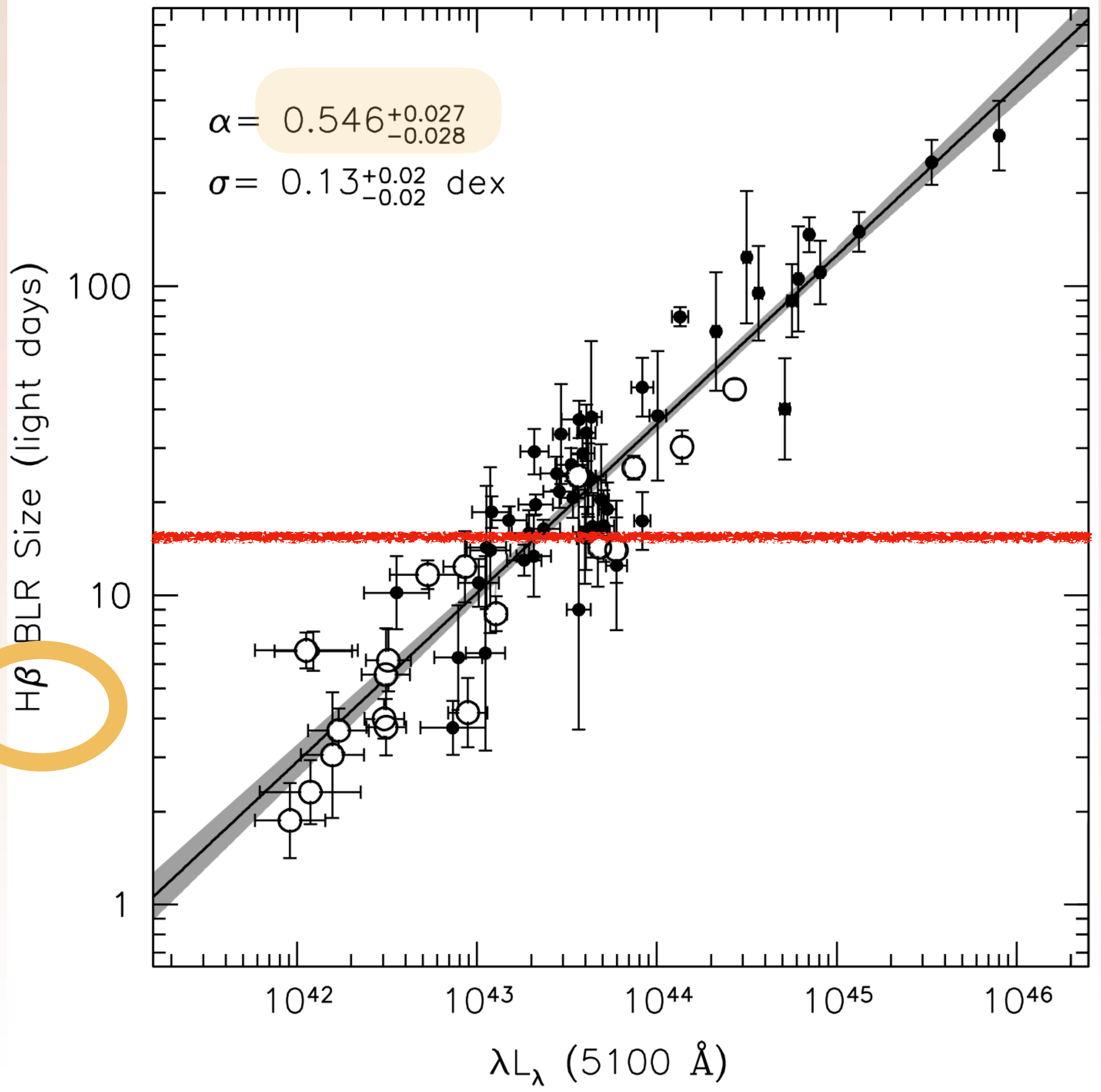

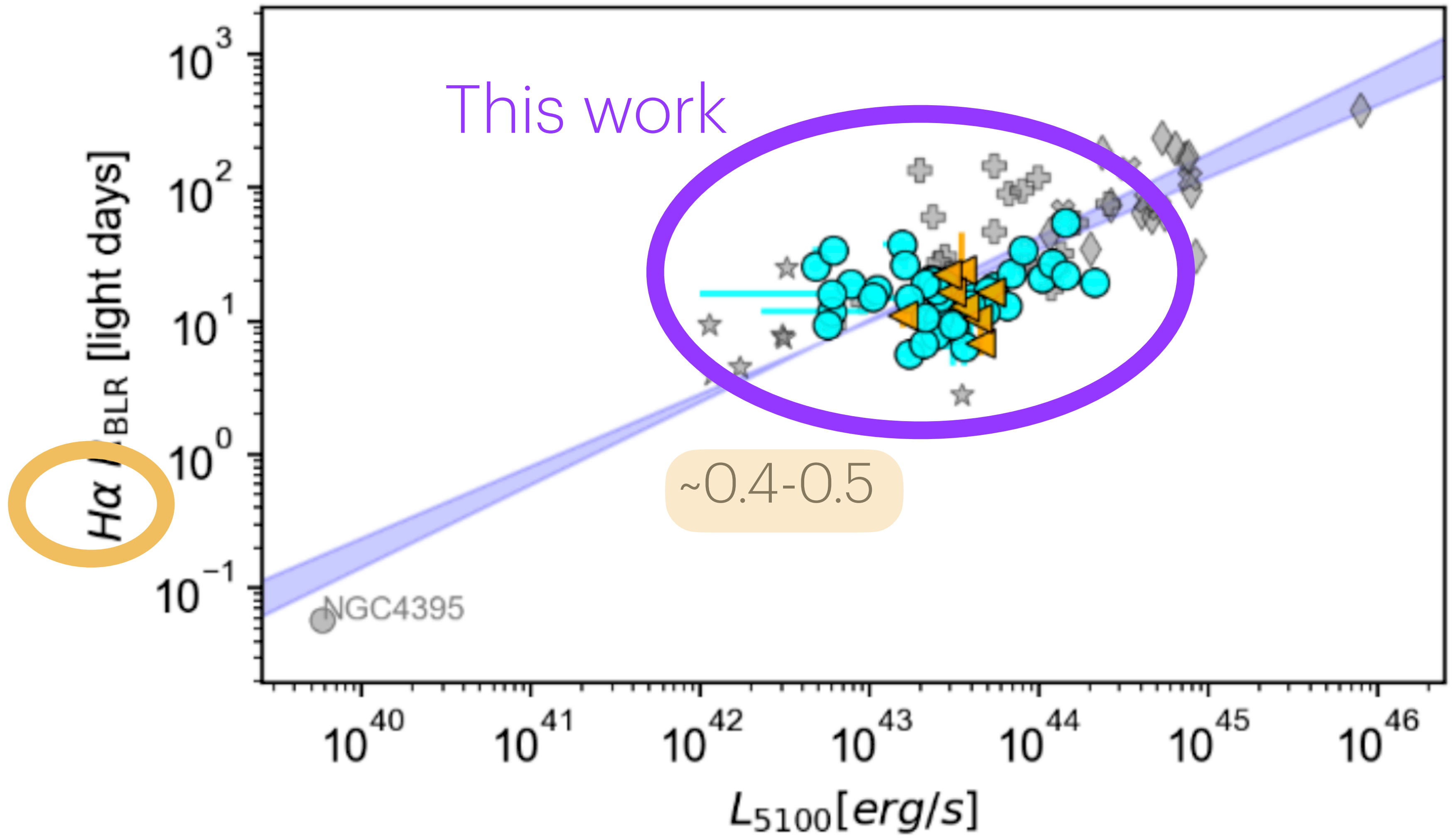

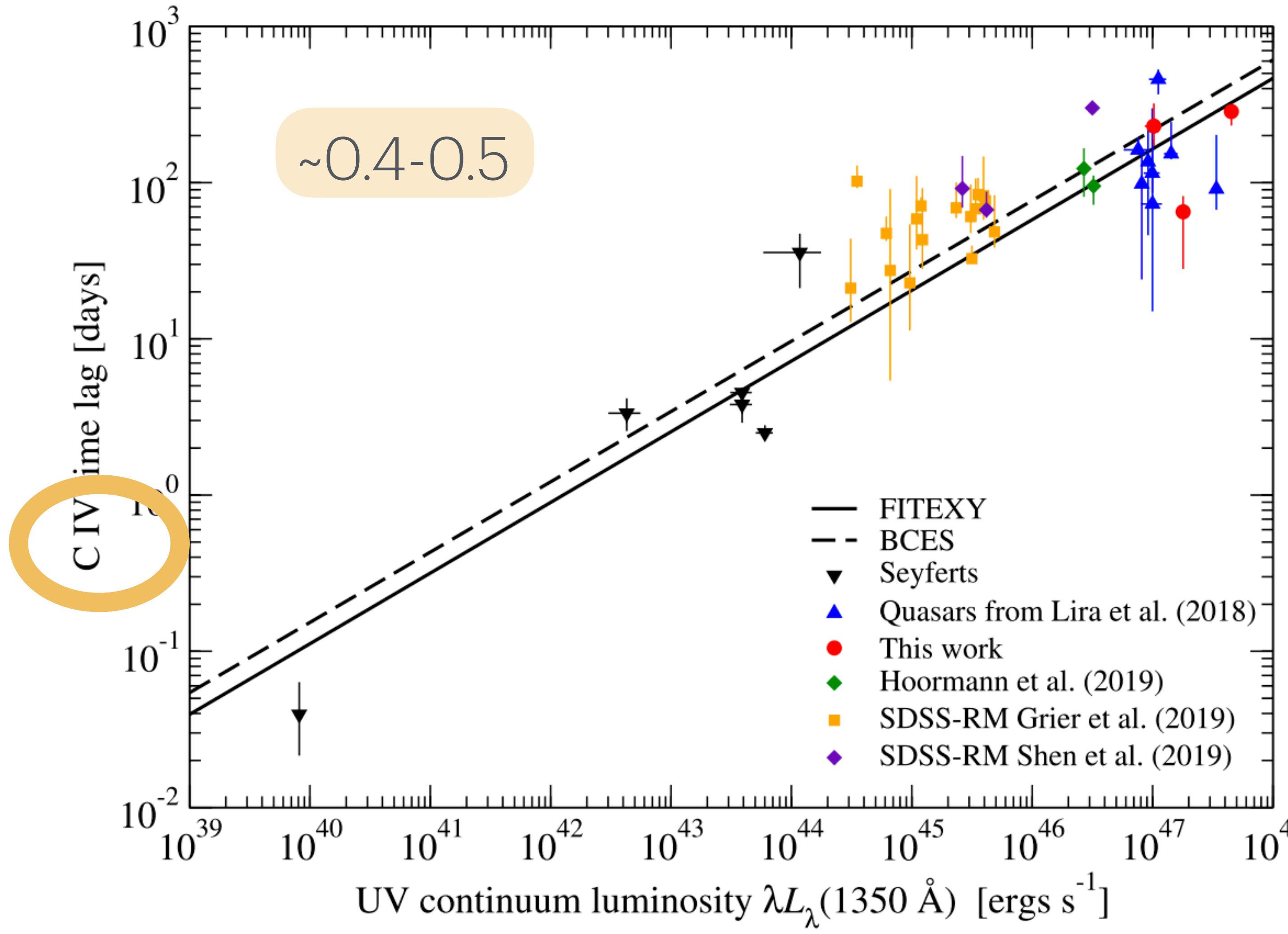

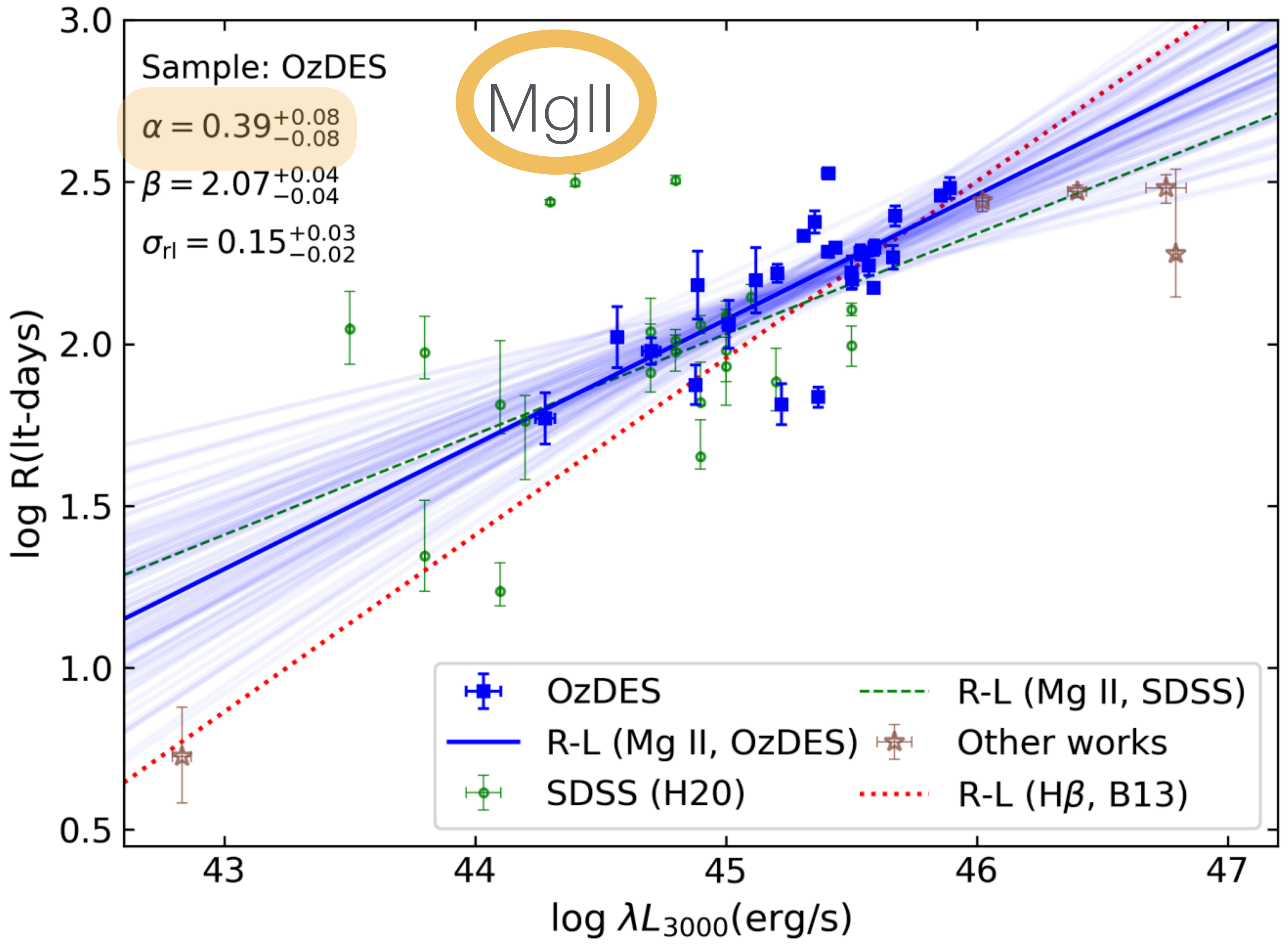

Backup

Light curve quality

Von Neumann $\hat{\sigma}^2_{vN} = \frac{1}{2(n-1)} \sum_{i=1}^{n-1} (X_{i+1} - X_i)^2$

Variance $s^2 = \frac{1}{n-1} \sum_{i=1}^{n} (X_i - \bar{X})^2$

Definition of $\eta = \sigma^2 / s^2$

Confidence level

Randomly shift light curve data

Probability to get this time delay and alpha for random data

Backup

Time delay determination: τ-α formalism: Simulations

Simulations:

- Test formalism with simulated light curves
- Compare results to widely used ICCF:
  ICCF start showing smaller delays for α < 0.6
- Delay well recovered until α ~ 0.2
  20% varying component
- Depending on sampling and noise: α well
  recovered until 0.3, then overestimated

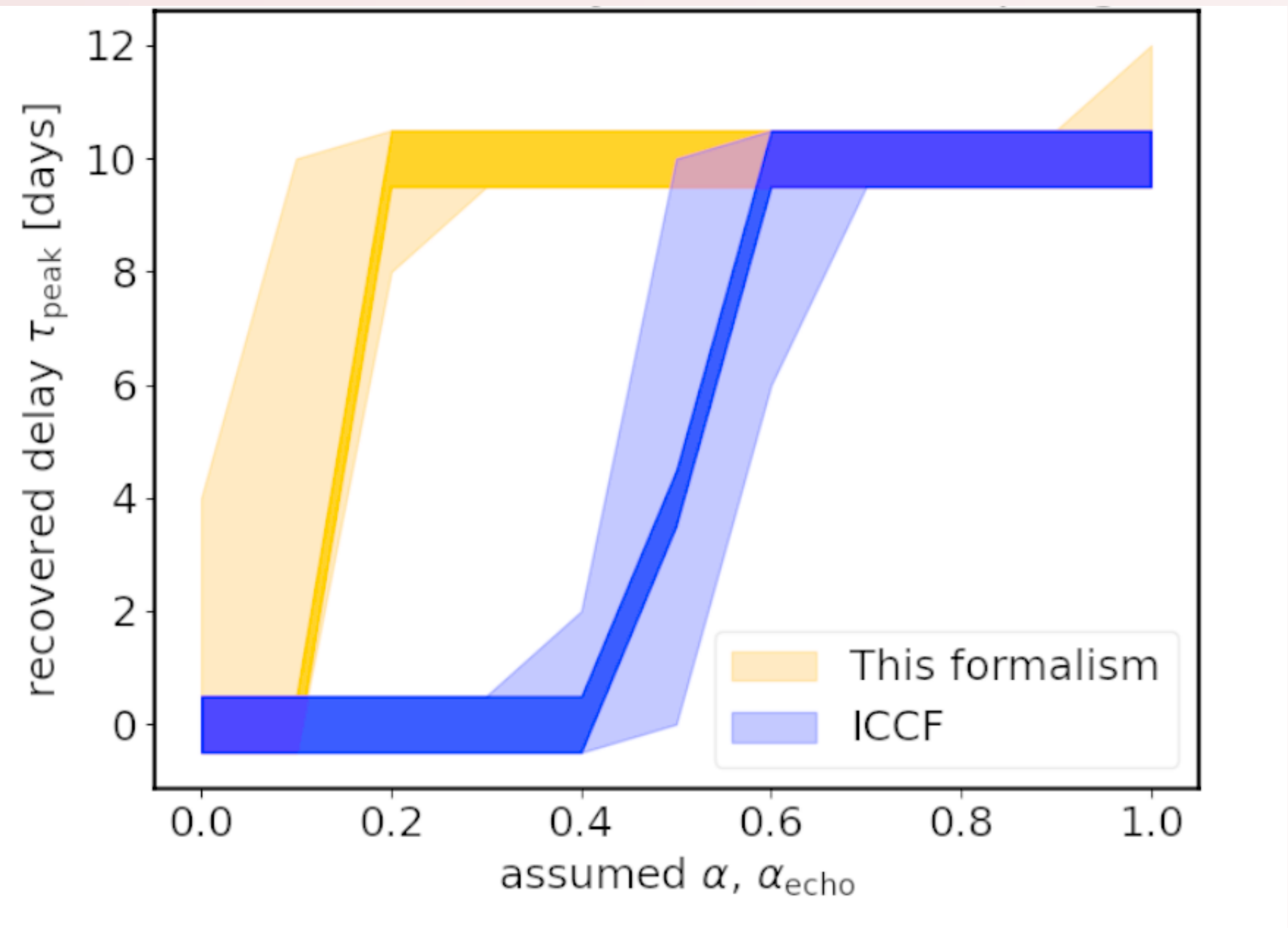

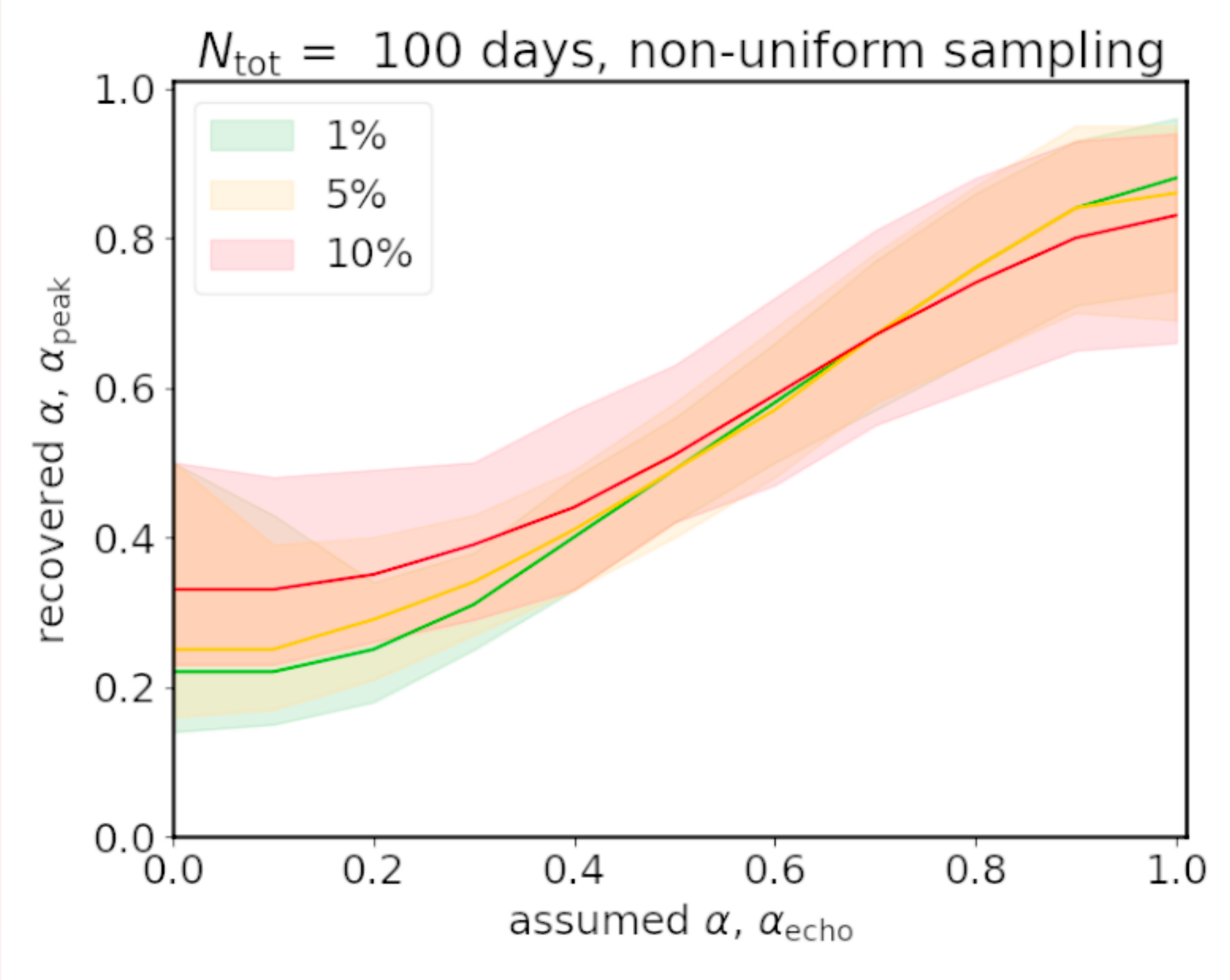

Radius — Luminosity Relation

Scatter

- BLR size and AGN geometry: foreshortening effect (observe shorter
  delays) if the BLR clouds are located near the observer
- Material between AD and observer within AGN affects the AGN luminosity
- Multi-epoch lag-luminosity scatter: which is the 'stable' BLR size/luminosity?
- Changing Look AGN, affect the r-L calibration
- Accretion rate plays a role
- Another estimations for the accretion rate,
  like done for Hbeta with R_{Fe}
- Improve r-L calibration for Cosmology parameters

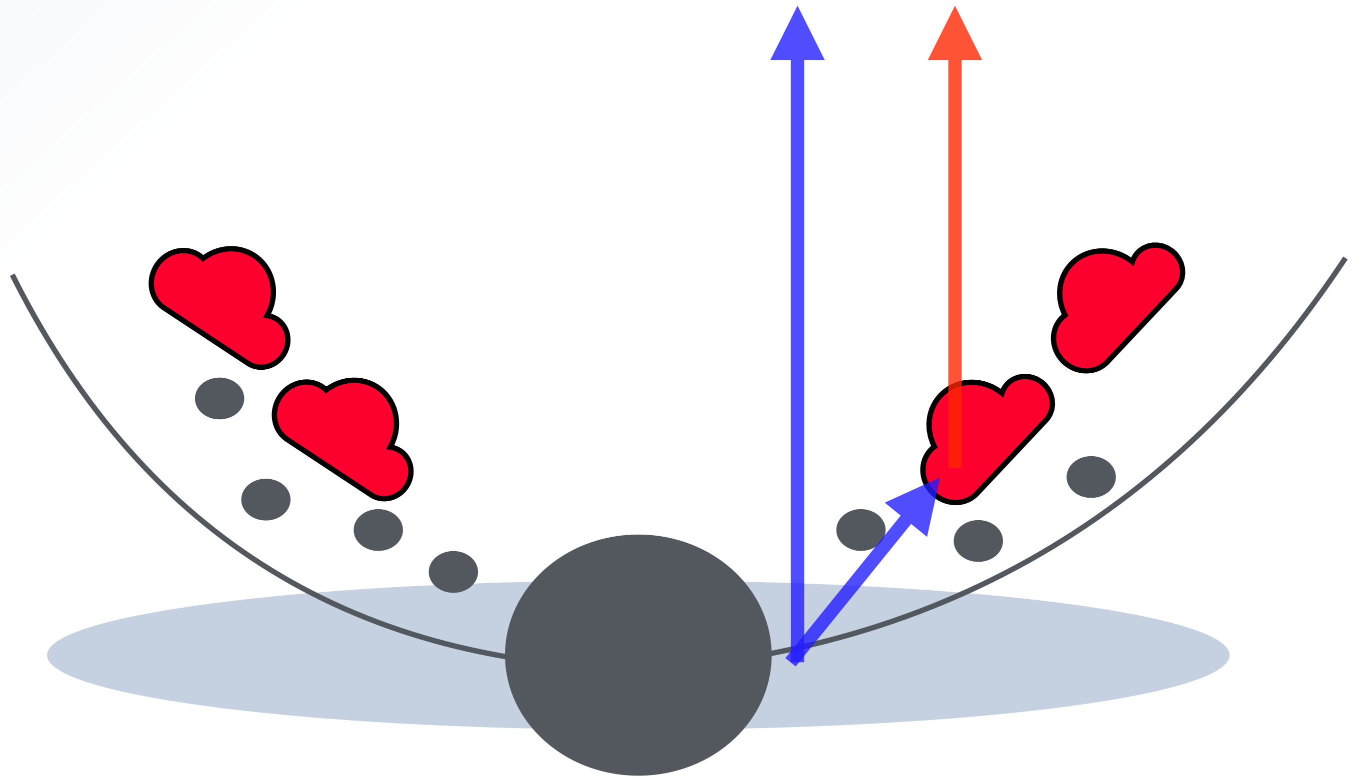

Hβ Compilation